(15)

NORDA Report 45

NOAA-7 AVHRR Images Obtained During the Iberian Var Experiment in the Alboran Sea, 1—20 October 1982

Michèle Champagne-Phillippe*
Paul E. La Violette

Ocean Science Directorate
Ocean Sensing and Prediction Division

February 1984

*Etablissement d'Etudes et de Recherches de la Météorologie.
Centre de Météorologie Spatiale
Lannion, France

Naval Ocean Research and Development Activity
NSTL Station, Mississippi 39529

Foreword

This report documents a portion of the joint French/United States investigation of the Alboran Sea. This portion deals with the satellite data received during 1-20 October 1982. The scientific purpose of the satellite data collection was to provide synoptic thermal coverage of the Alboran Sea, particularly in the region of the incoming Atlantic water near the Strait of Gibraltar.

G. T. Phelps, Captain, USN
Commanding Officer, NORDA

Executive Summary

During the period 1-20 October 1982, NOAA-7 satellite data were received and archived at Centre de Meteorologie Spatiale (CMS), Lannion, France. These data were collected as part of the multi-platform international experiment called ¿Donde Va?. The scientific purpose of the satellite data collection was to provide synoptic thermal coverage of the Alboran Sea particularly in the region of the incoming Atlantic water near the Strait of Gibraltar. This report presents comparatively cloud-free images for use as an aide in the analysis of ¿Donde Va? multi-platform data collected by other members of the ¿Donde Va? investigative team. All of the images presented are registered to a Mercator projection. In addition, the infrared images have been atmospherically corrected to minimize the effects of atmospheric moisture. The visible images have been enhanced to show sea surface roughness and turbidity changes.

Acknowledgments

The authors wish to acknowledge the assistance of the computer scientists and photographers of Centre de Metrologie Spatiale and Ramon A. Oriol of the Naval Ocean Research and Development Activity in the realization of the images presented in this report. Mr. La Violette's portion of ¿Donde Va? was sponsored under a contract with the Office of Naval Research, Code 422, Coastal Studies; Dennis Conlin, program manager.

NOAA-7 AVHRR Images Obtained During the ¿Donde Va? Experiment in the Alboran Sea, 1-20 October 1982

1. General

During the period 1-20 October 1982, NOAA-7* satellite data were received and archived at Centre de Meteorologie Spatiale (CMS), Lannion, France. These data were collected as part of the multi-platform international experiment called ¿Donde Va?.** The scientific purpose of the satellite data collection was to provide synoptic thermal coverage of the Alboran Sea particularly in the region of the incoming Atlantic water near the Strait of Gibraltar. This report presents comparatively cloud-free images for use as an aide in the analysis of ¿Donde Va? multi-platform data collected by other members of the ¿Donde Va? investigative team.

2. The NOAA-7 Data

The archived data are NOAA-7 High Resolution Picture Transmission (HRPT) digital data recorded by the Advanced Very High Resolution Radiometer (AVHRR) in five wavelength ranges. The characteristics of the AVHRR are given in Table 1. More information on the NOAA satellites and the AVHRR sensor may be found in Schwalb (1978) and Hussey (1979).

3. Processing

The raw data are achived on 1600 BPI tapes at both CMS and NORDA. At NORDA these data were calibrated and then registered to a Mercator projection of the Alboran Sea (see Appendix I). The infrared data were then corrected for atmospheric absorption effects using an algorithm developed by Deschamps and Phulpin (1980) and adjusted by Phulpin, at CMS. This algorithm uses a combination of channels 4 and 5 of the NOAA-7 AVHRR (see Appendix II).

4. The Visible and Infrared Images

The NOAA-7 AVHRR images containing too much cloud cover were not processed. Of the total images examined, data from 30 orbits (Table 2) were sufficiently cloud free to form usable images for presentation in this report. Both visible and infrared images are shown for the daylight orbits. In the visible images (channel 1), the less reflective areas (i.e., the sea) are represented with the lighter shades of gray. Since the enhancements were made to display changes in the lightness of cloud free sea surfaces and not to make cloud classification, most of the clouds appear black saturated. The infrared image shows the corrected sea surface temperatures (SST) obtained from the combination of channels 4 and 5. The SST images use the conventional IR representation with the warmest waters represented by dark gray tones and the coldest appearing as the lightest gray tones. For night orbits, only the SST image is presented. The times of the night orbits are approximately 0300 hours (UT), whereas the day orbits are around 1500 hours (UT). Thus, a given day's night image will proceed the day image in the order of images presented here.

Beyond the brief remarks presented with the imagery no oceanographic analysis are included in this data report. An example of the oceanographic results obtained from using these data can be found in La Violette (1983).

*National Ocean and Atmospheric Administration

**The primary objective of ¿Donde Va? was to measure the velocity and hydrographic structure of the incoming flow of Atlantic water. A full description of the rational and the data collection approach to the experiment can be found in the "¿Donde Va? Operation Plan." A limited number of copies are available for individual requestors.

Table 1. NOAA-7 AVHRR characteristics

- scanning angle: 55°
- swath width: about 3000 Km
- spatial resolution: 1.1 Km at sub-point, 4 Km at the edges
- equivalent temperature noise (NE T) :0.12° K at 300° K (Channels 4 and 5)

Channel	Spectral range (m)	Main applications
1	0.55-0.70	Daylight cloud analysis. Land applications
2	0.70-1.10	Land sea discrimination. Land applications
3	3.55-3.93	Sea surface temperatures. Nighttime cloud discrimination
4	10.3-11.3	Sea surface temperatures. Nighttime cloud analysis
5	11.5-12.5	Sea surface temperatures. Nighttime cloud analysis

Table 2: List of NOAA-7 AVHRR data obtained during ¿Donde Va?

Orbit Number	Date (Oct. 82)	Time (UT)	Available Vis	Available IR	Orbit Number	Date (Oct. 82)	Time (UT)	Available Vis	Available IR
6560	1	0409		X	6701	11	0349		X
6567	1	1532			6708	11	1513	X	X
6574	2	0356		X	6715	12	0337		X
6581	2	1520			6722	12	1501	X	
6588	3	0345		X	6729	13	0325		X
6595	3	1508	X	X	6736	13	1449	X	
6602	4	0333			6743	14	0313		X
6609	4	1456	X	X	6750	14	1437		
6616	5	0320			6757	15	0301		X
6623	5	1444			6764	15	1425		
6630	6	0308		X	6771	16	0249		X
6637	6	1432	X	X	6778	16	1413	X	
6644	7	0256		X	6785	17	0236		X
6651	7	1420	X	X	6792	17	1400	X	X
6658	8	0244		X	6800	18	0406	X	X
6665	8	1408	X		6807	18	1530	X	X
6672	9	0232		X	6814	19	0354		X
6679	9	1356			6821	19	1518	X	X
6687	10	0402		X	6828	20	0345		X
6694	10	1526	X	X	6835	20	1505		

Figure 1. 1 October 1982, night IR. Disturbed pattern of the Alboran Sea gyre. The main warm core of the Alboran gyre (A, Tmax=22°C) is to the southeast and a cold feature appears between this warm core and the Gibraltar Strait.

Figure 2. 2 October 1982, night IR. Both the warm (A) and cold (B) core eddies have shifted a little to the southeast from their position on 1 October.


a

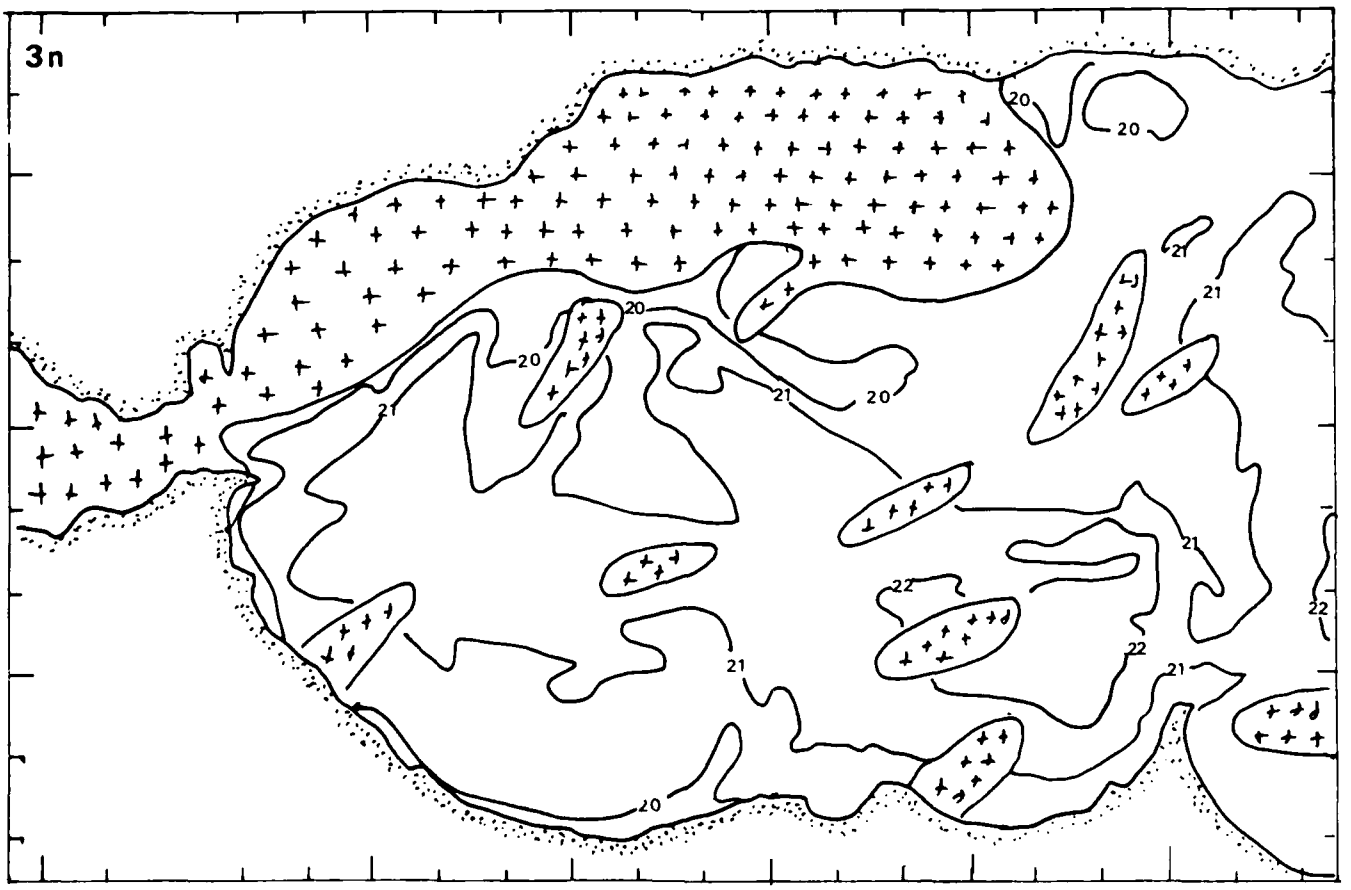
3n
20
20
20
20
21
21
20
21
21
22
22
21
22
21
20

Figure 5. 3 October 1982, day VIS. Clouds obscure the southern part of the Alboran Sea. Isolated clouds can also be seen along the Spanish coast.

Figure 3. 3 October 1982, night IR. SST gradients have begun to weaken and appear more confused (*a*: Tmax=22°C; Tmin probably under clouds). Some clouds appear black on this corrected image. This effect will be noticeable in many of the IR images which follow. It is due to a large positive difference between their temperatures at 11 and 12 μm. (Top of previous page.)

Figure 4. SST chart corresponding to 3 October 1982, night IR image. (Bottom of previous page.)

Figure 6. 3 October 1982, day IR. SST gradients remain weak outside the eastern part of the Gibraltar Strait area. (Tmax >22.5°C probably below the clouds; Tmin <18°C at A. At C temperatures range between 19 and 20.5°C). (Top of opposite page.)

Figure 7. SST chart corresponding to 3 October 1982, day image. (Bottom of opposite page.)


C

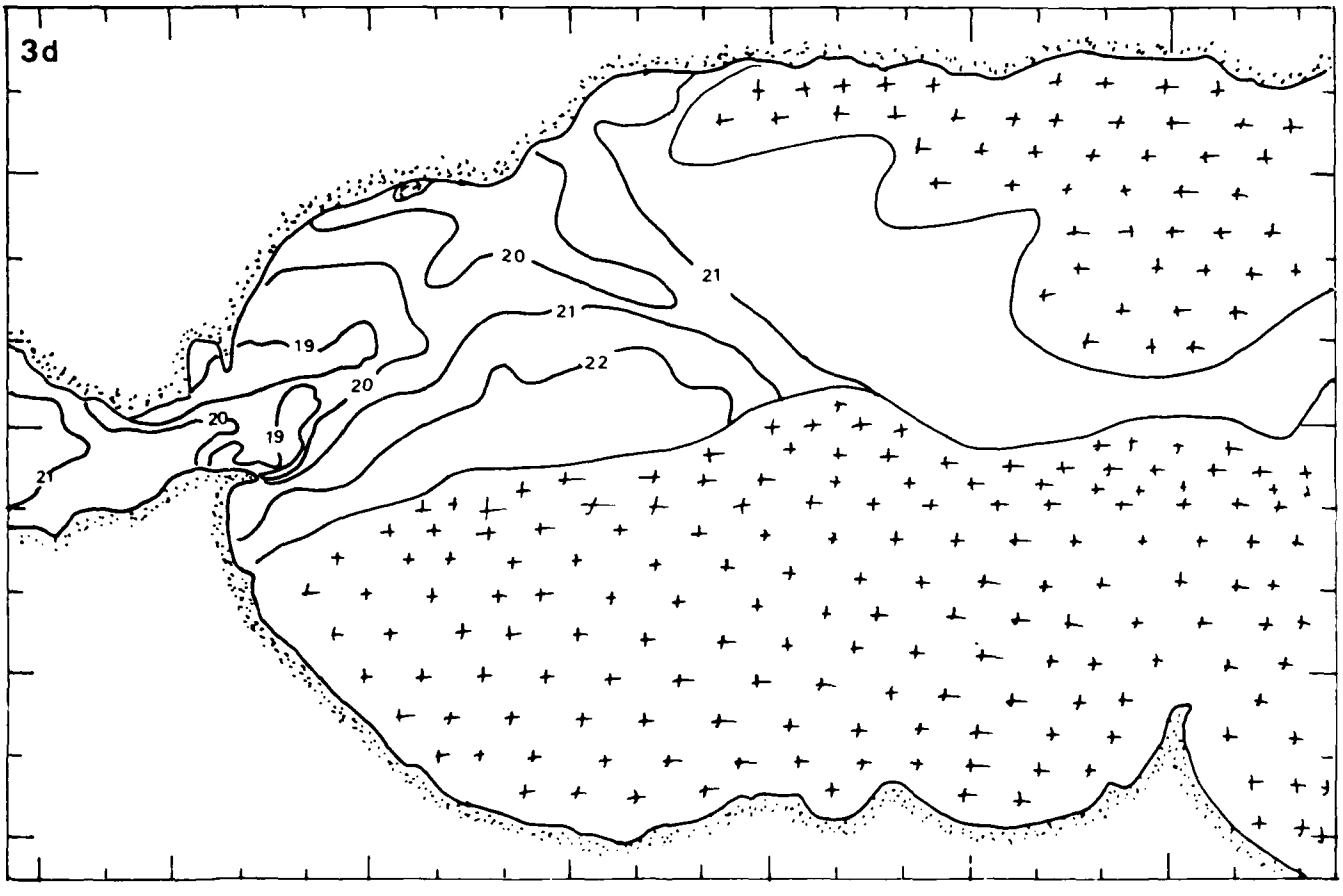
3d
20
21
19
20
22
20
19
21

Figure 8. 4 October 1982, day Vis. Cloudy.

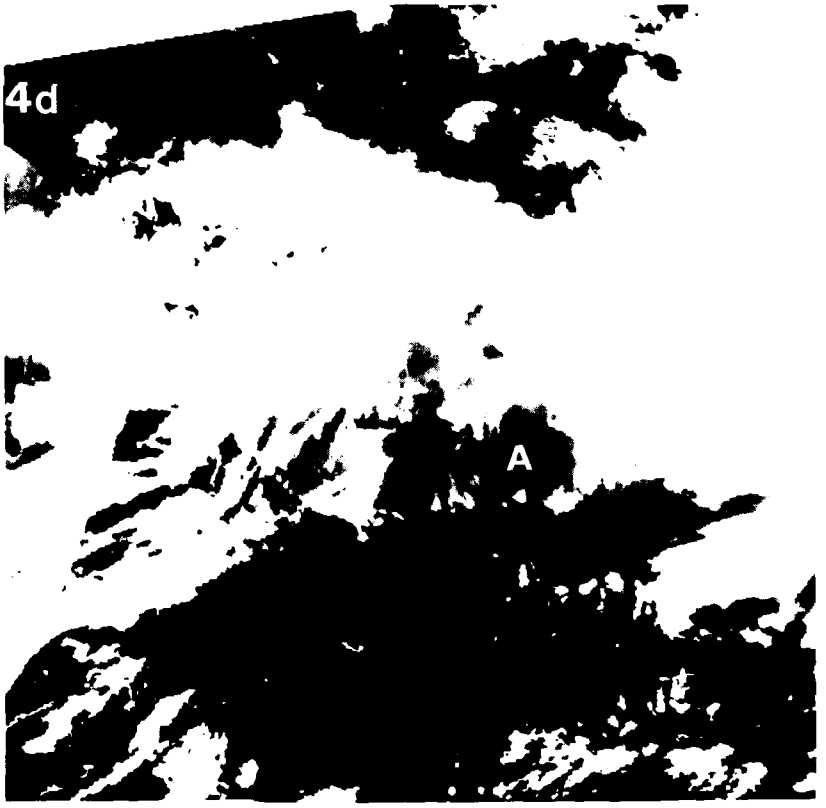

Figure 9. 4 October 1982, day IR. The image is sufficiently cloudy so that SST gradients cannot be well detected. (At A, temperatures ranged between 22.5 and 23°C).

Figure 10. 6 October 1982, night IR. The storm of 5 October and an onset of strong westerly winds have evidently induced sufficient surface mixing to cause a rapid decrease of sea surface temperatures (Tmax=21.5°C; Tmin=15.5°C at A). Notice that the image seems to be blurred by fine clouds.

Figure 11. 6 October 1982, day Vis. A bright "plume" (dark in the image) appears to prolongate from the Gibraltar Strait into the Alboran Sea. It seems to coincide with the area where the prevailing northwesterly winds are channeled into a west to east direction by the mountains on each side of the Strait of Gibraltar. Since this rather large phenomenon doesn't appear in the uncorrected IR images, it may be inferred that it is due to an increase in the roughness of the sea in this bright area. Notice that the northern edge of the plume is sharper than the southern one and that this edge coincides with the northern limit of the Atlantic jet (see Fig. 12). Superimposed on these features lies an intricate network of lee-waves with a weaker signature than the Gibraltar rough-water plume.

Figure 12. 6 October 1982, day IR. The atmospheric effects apparent in the visible image of Figure 11 do not appear in this companion IR image. In comparison to the previous days, the average SST in the Alboran Sea has decreased with the SST gradients appearing to have increased. This is probably due to active wind mixing and the horizontal and vertical movements of the water. A patch of warm water (i.e. warmer than 21°C) remaining from the previous days is surrounded by colder upwelled waters. The coldest temperatures (<17°C) are observed as usual in the Gibraltar-Marbella area with temperatures lower than 16° C occurring at A. (Top of opposite page.)

Figure 13. SST chart corresponding to 6 October 1982, day IR image. (Bottom of opposite page.)

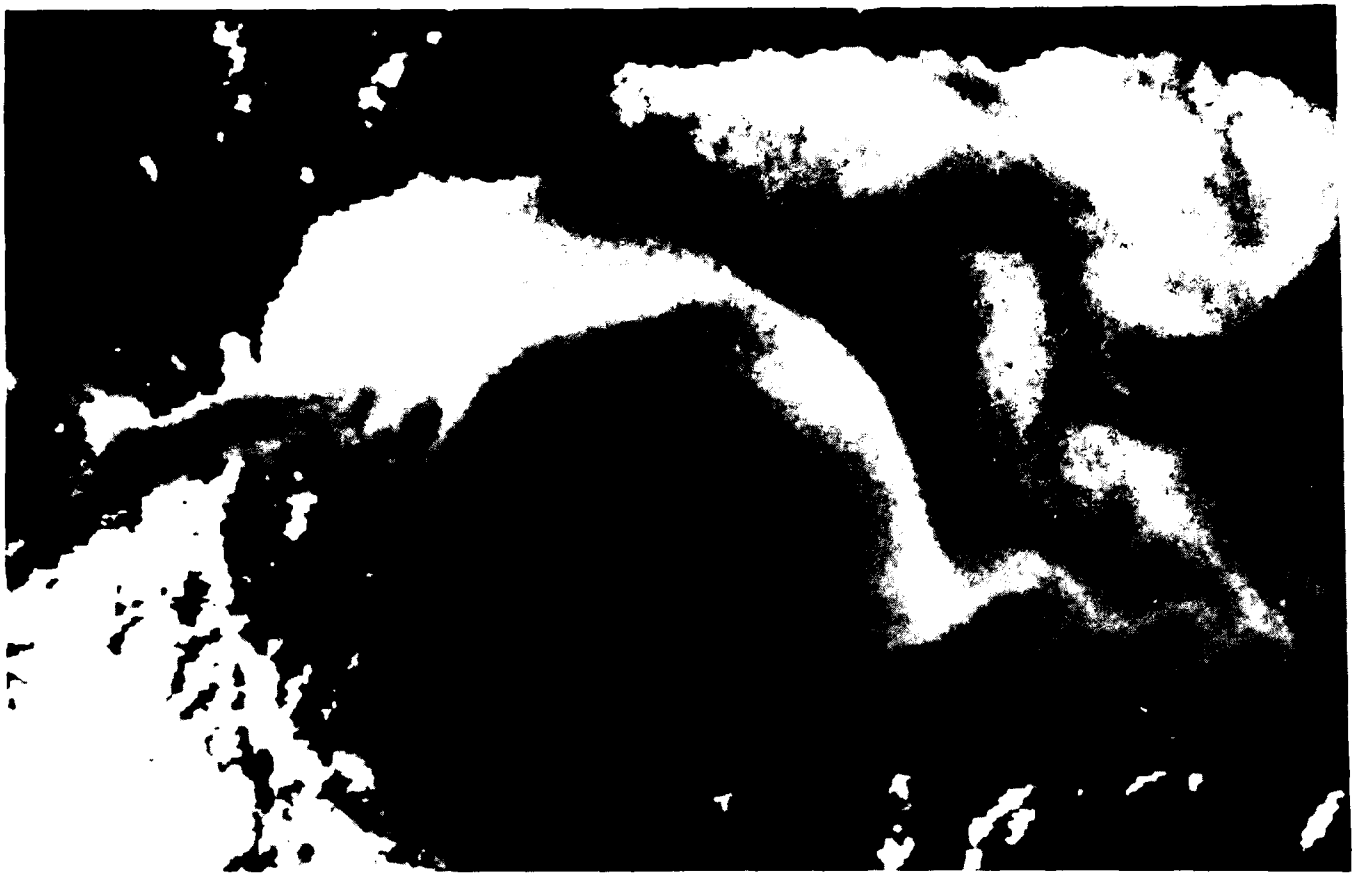

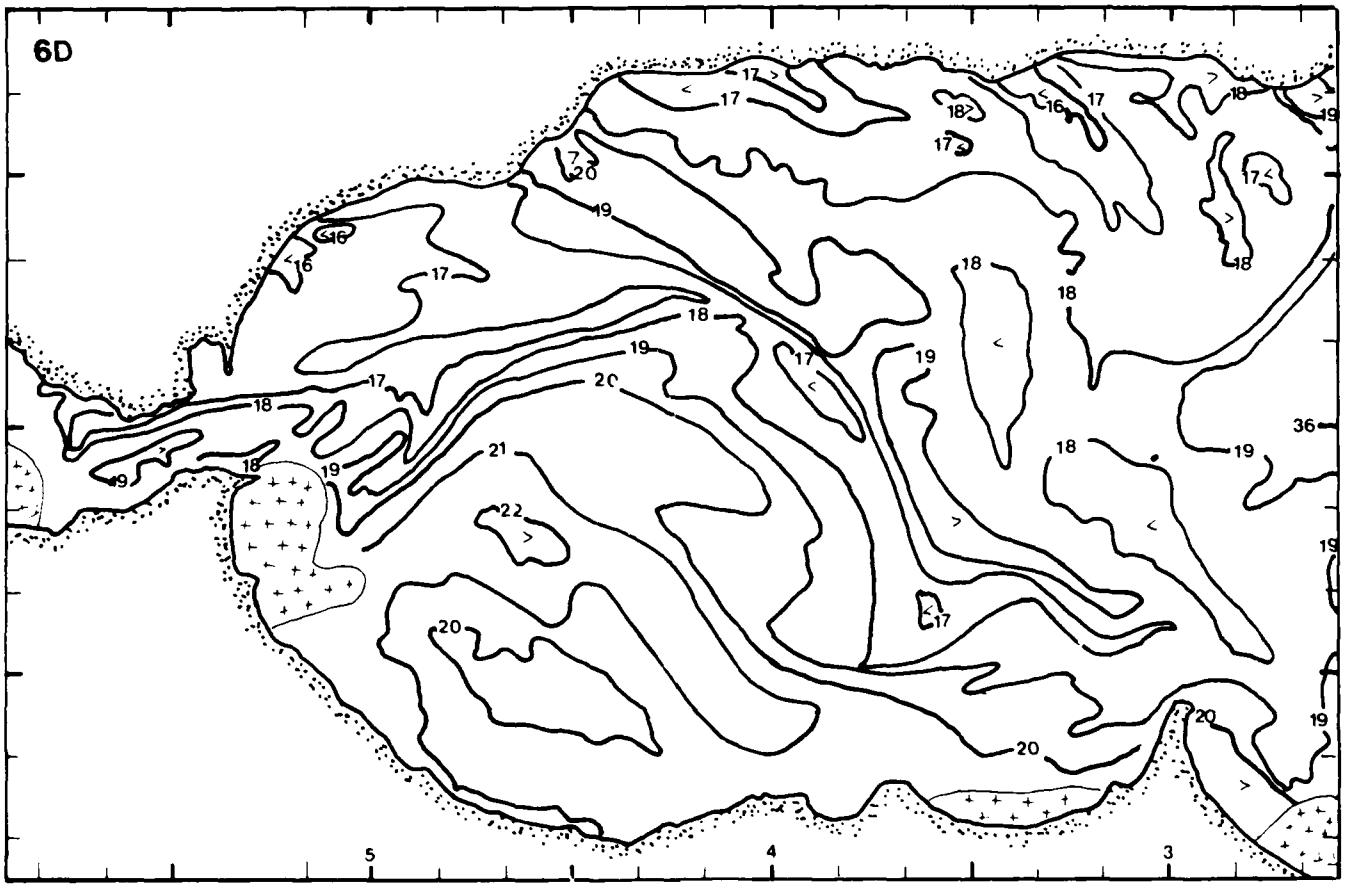
6D
17
16
18
19
20
21
22
36
5
4
3

Figure 14. 7 October 1982, night IR. The pattern is similar to the one observed 12 hours earlier (Figure 12). SST are lower, probably due to the night radiative cooling. (Top opposite page.)

Figure 15. SST chart corresponding to 7 October 1982, night IR image. (Bottom opposite page.)

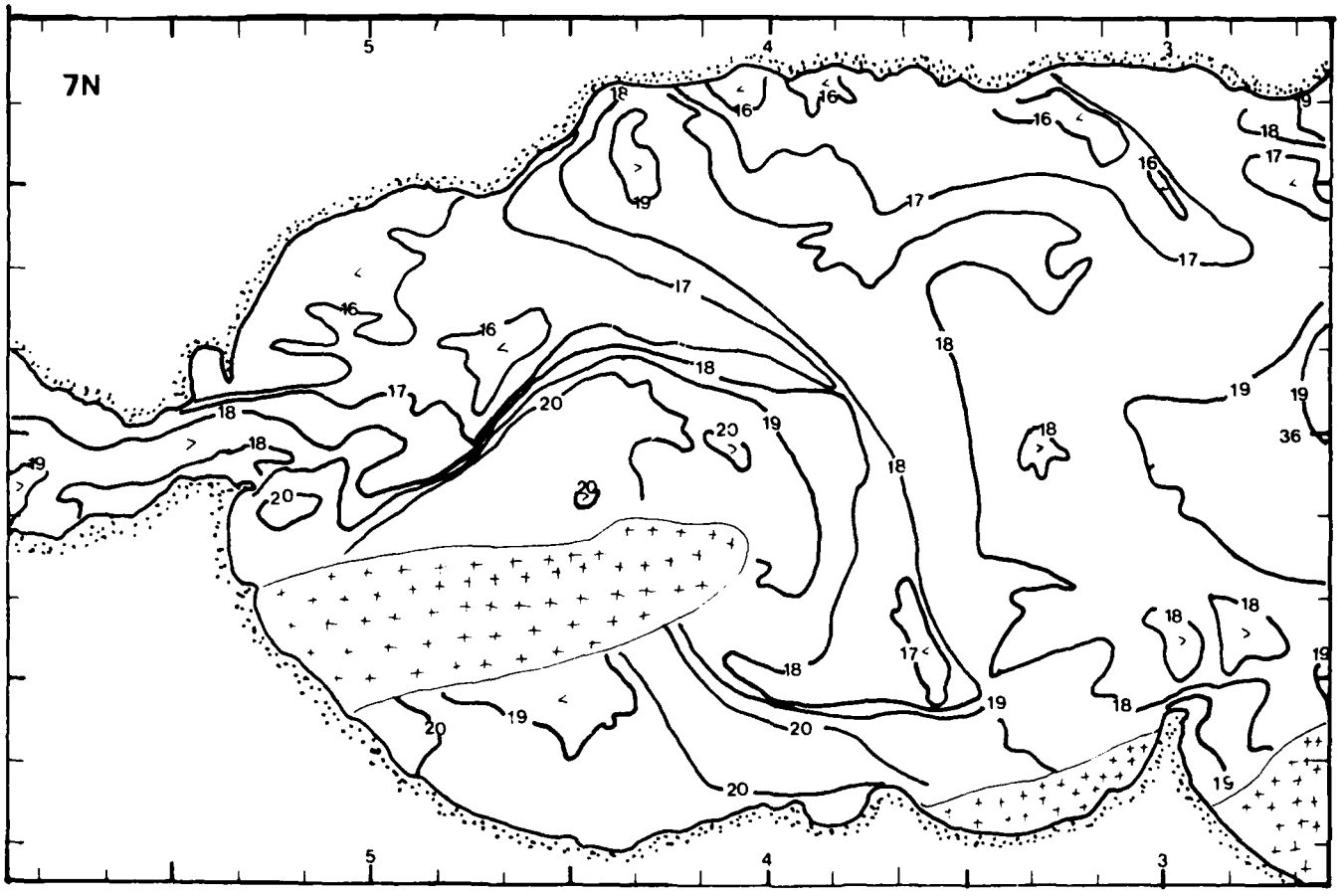
7N
5
4
3
16
17
18
19
20
36

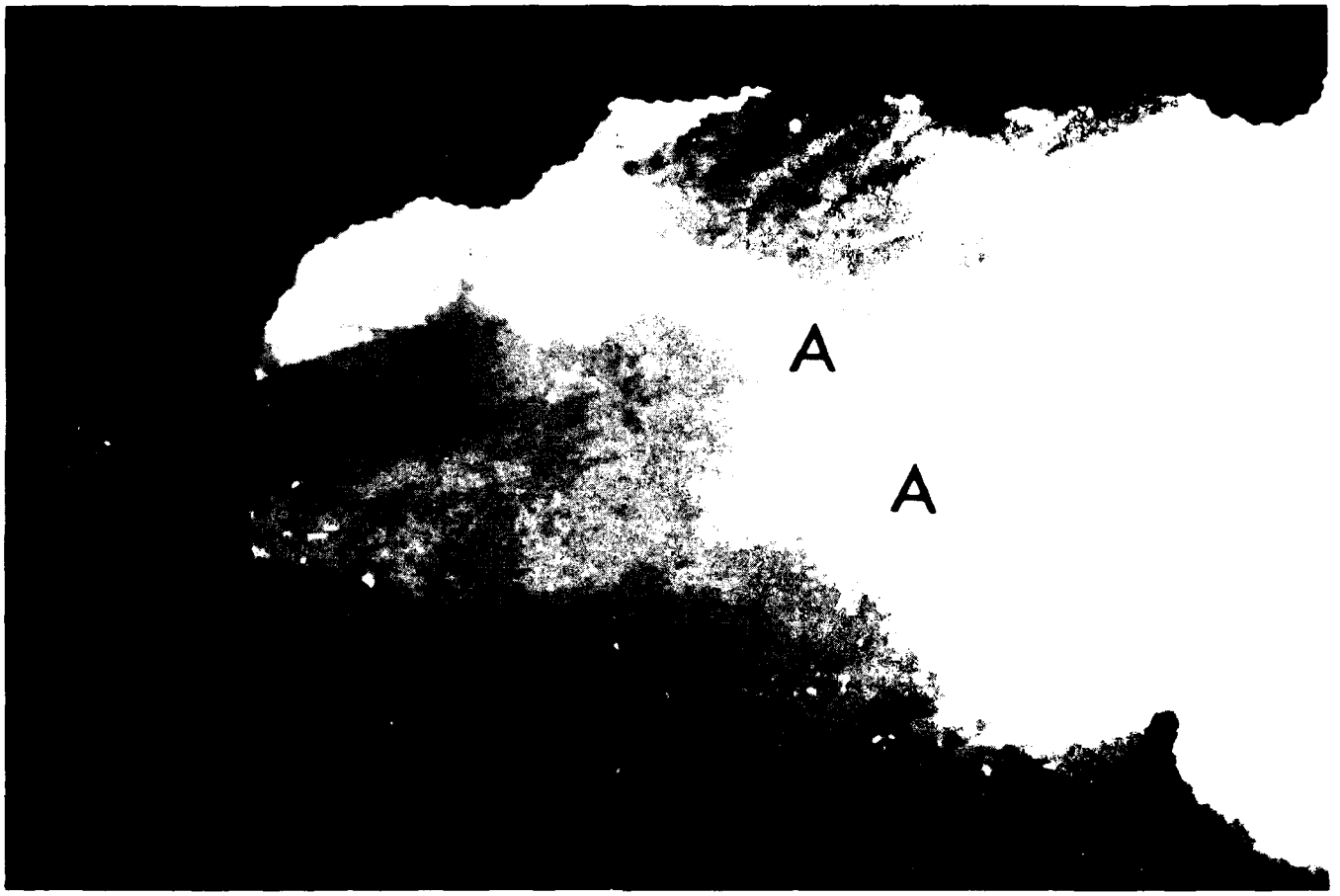

Figure 16. October 1982, day Vis. A "plume" of bright waters, less marked than on 6 October 1982, appears to still be prolongated out from the Strait of Gibraltar. Notice the less reflective strip (A) that outlines the coldest part of the Atlantic jet around its northeastern area. Notice also the equally less-reflective area which corresponds to the region of cold water in the Gibraltar-Marbella area.

Figure 17. 7 October 1982, day IR. With only some slight changes, the thermal features are generally similar to those observed during the previous passes. Temperatures are about 0.5°C higher than on the night of 7 October, which may be a diurnal effect but they are also about 1°C colder than on 6 October. The main front (B) is very sharp with a maximum gradient reaching 3°C in less than 3 km.
(Top opposite page.)

Figure 18. SST chart corresponding to the 7 October 1982, day IR image.
(Bottom opposite page.)


A
B
A

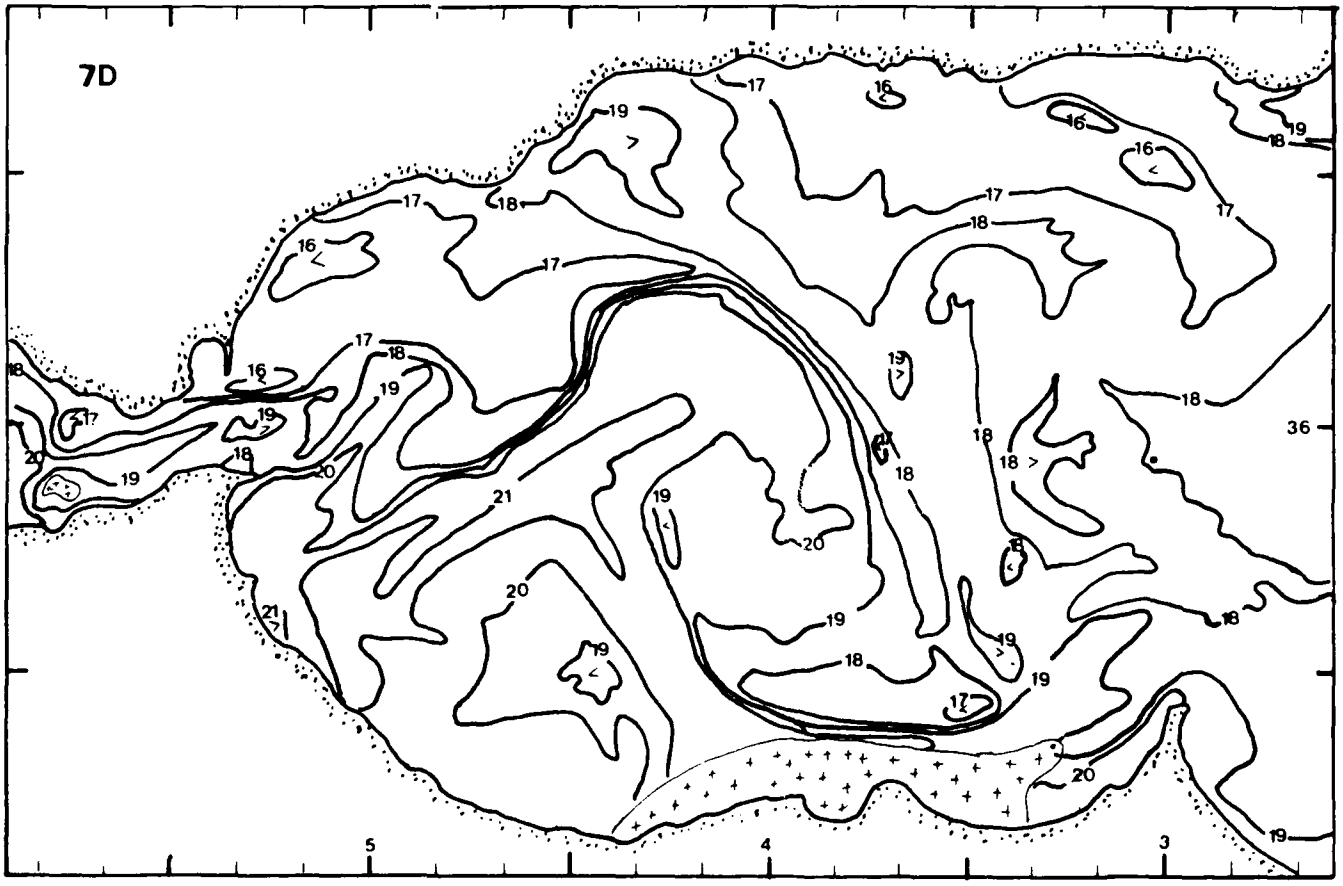
7D
5
4
3
36

Figure 19. 8 October 1982, night IR. The main thermal features again are similar to those observed on the previous days. The SSTs show an average decrease from 7 October (day) of about 1.5 to 2.0°C and about 1°C less than 7 October (night). While this may be due to the continuation of meteorological and diurnal effects, it is more than likely due to this image lying near the edge of the AVHRR swath. In the regions near the edge of the swath, the look angle is so large that the linear correction algorithm may no longer be considered accurate. (Top opposite page.)

Figure 20. SST chart corresponding to the 8 October 1982, night IR image. (Bottom opposite page.)

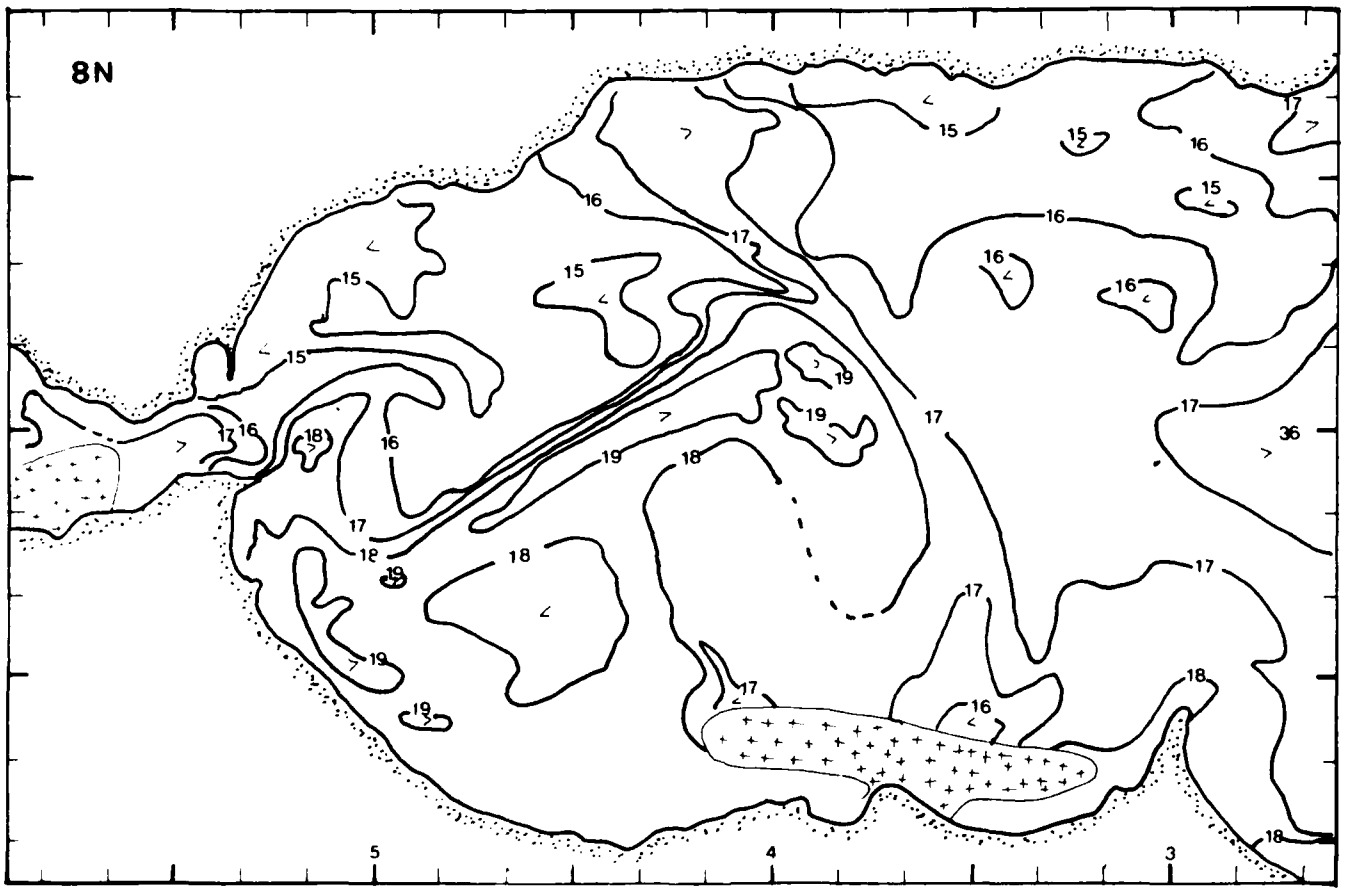
8N
15
16
17
18
19
36
5
4
3

Figure 21. 8 October 1982, day Vis. Image blurred by clouds. Notice at A, the less-reflective features correspond to cold water regions in the companion IR image.

Figure 22. 8 October 1982, day IR. The sharp front induced at B during the previous days by the encounter between the warm "T-like" feature and the waters of the Atlantic jet is becoming weaker (a discussion on these submesoscale features can be found in La Violette, 1983). The main front between the Strait and 5°W is now located at C. The SST chart shows that temperatures have about the same values as on 7 October (day), but the temperature of the "T-like" feature has decreased from 21 to 20°C. (Top opposite page.)

Figure 23. SST chart corresponding to the 8 October 1982, day IR image. (Bottom opposite page.)


A
C A A

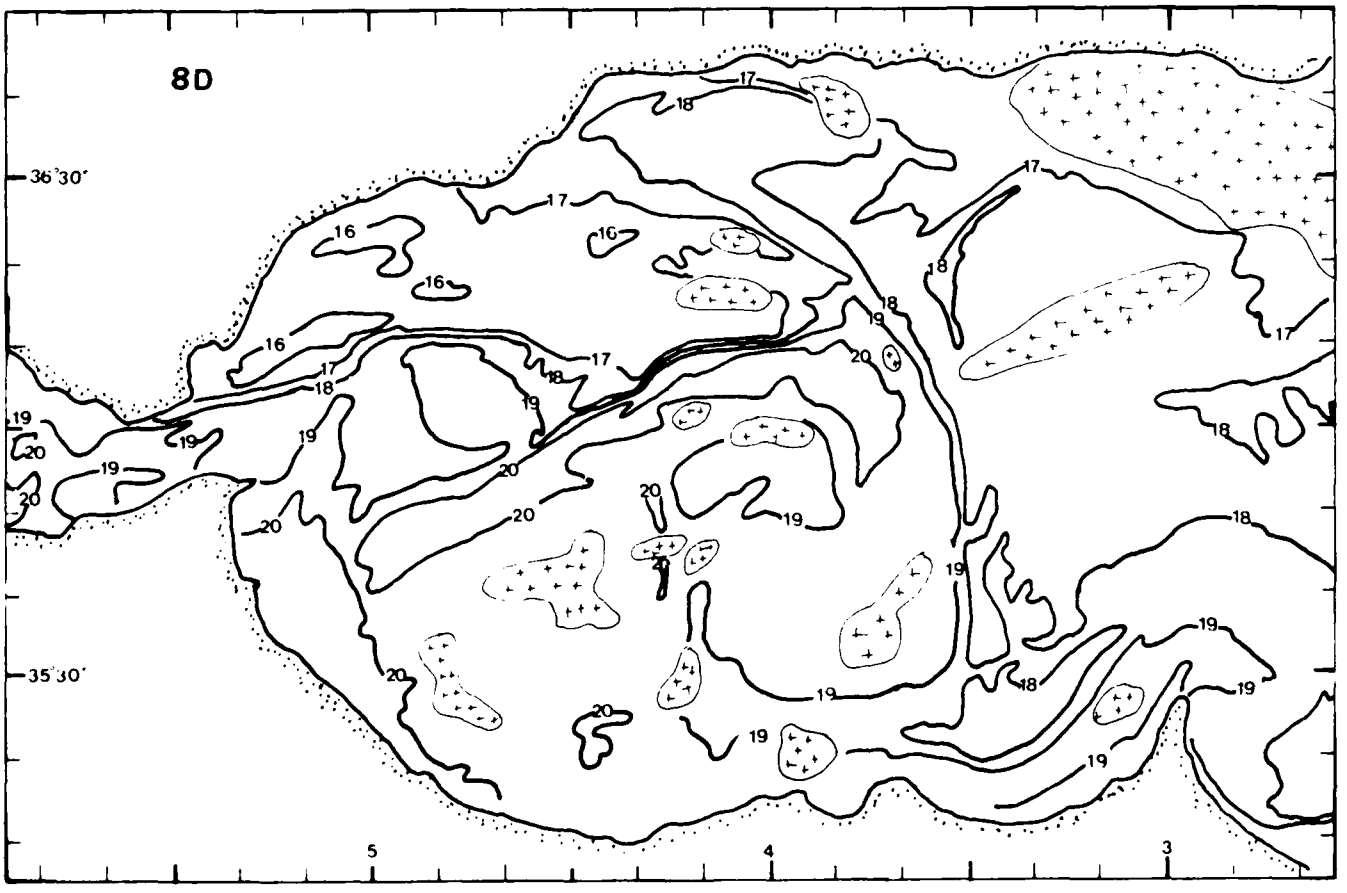
8D
36°30'
35°30'
5
4
3

Figure 24. 9 October 1982, night IR. This IR image located that the very edge of the AVHRR swath has the same problem as the 8 October (night) IR image. SST values range from 19°C at (a) to less than 14°C at (b) and these low values are probably due to an insufficient correction of AVHRR data. But, in situ comparative measurements are needed to make further comments on these low temperatures. (Top page 21.)

Figure 25. SST chart corresponding to the 9 October 1982, night IR image. (Bottom page 21.)

Figure 26. 10 October 1982, night IR. Althought the SST structure appears to be changing, clouds in the image prevent a good SST chart of the change. This image confirms the increasing importance of the frontal feature located at (C). (Top page 22.)

Figure 27. 10 October 1982, day Vis. This image, almost entirely cloud free, shows a very regular brightness pattern with the less reflective waters located southeast of the Strait of Gibraltar (A) and the more reflective waters being found along the coastlines. It is difficult to state whether this is the influence of turbidity or caused by increased sea surface roughness associated with the windier coastal regions on this otherwise calm day. (Bottom page 22.)

Figure 28. 10 October 1982, day IR. The "T-like" feature has translated eastward. The main surface front is now located at (A) and it is distrubed by wave-like features. SSTs remain low as indicated by the values on the SST chart. The image might be another example of "cooling" due to location of the study area close to the AVHRR swath edge. (Top page 23.)

Figure 29. SST chart corresponding to the 10 October 1982, day IR image. (Bottom page 23.)


B
B
A
A

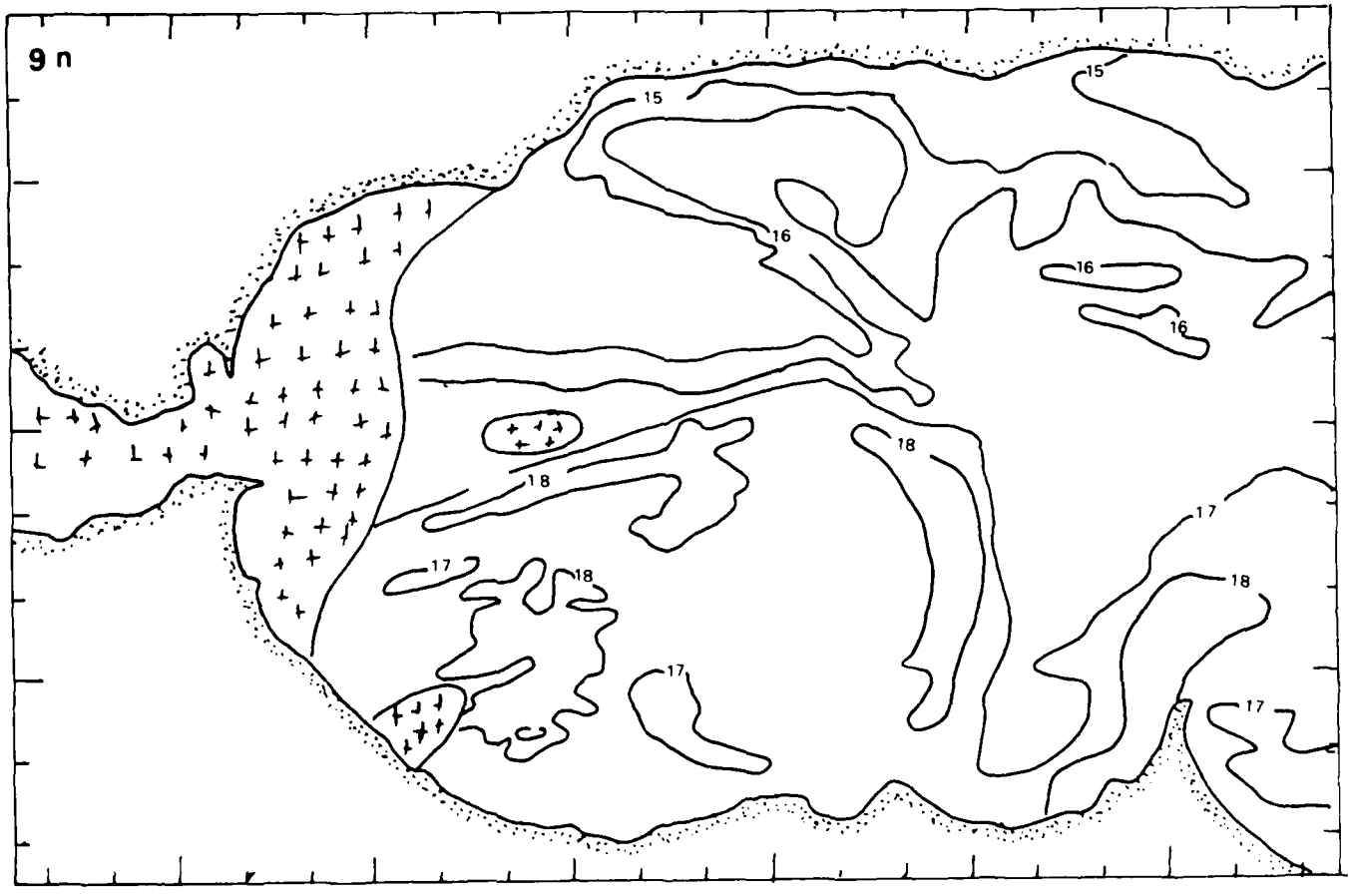
9 n
15
15
16
16
16
18
18
17
17
18
17
18
17

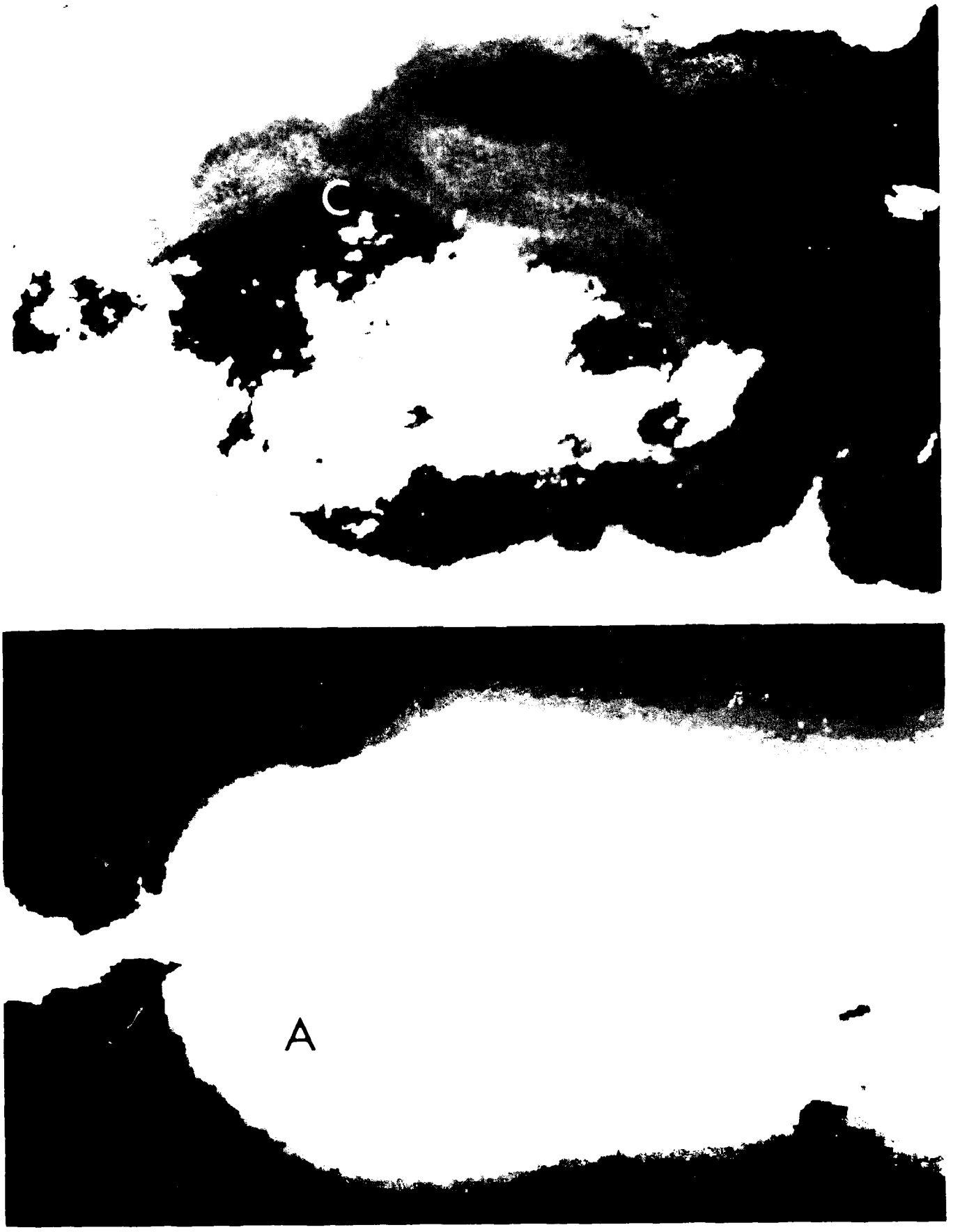
C
A

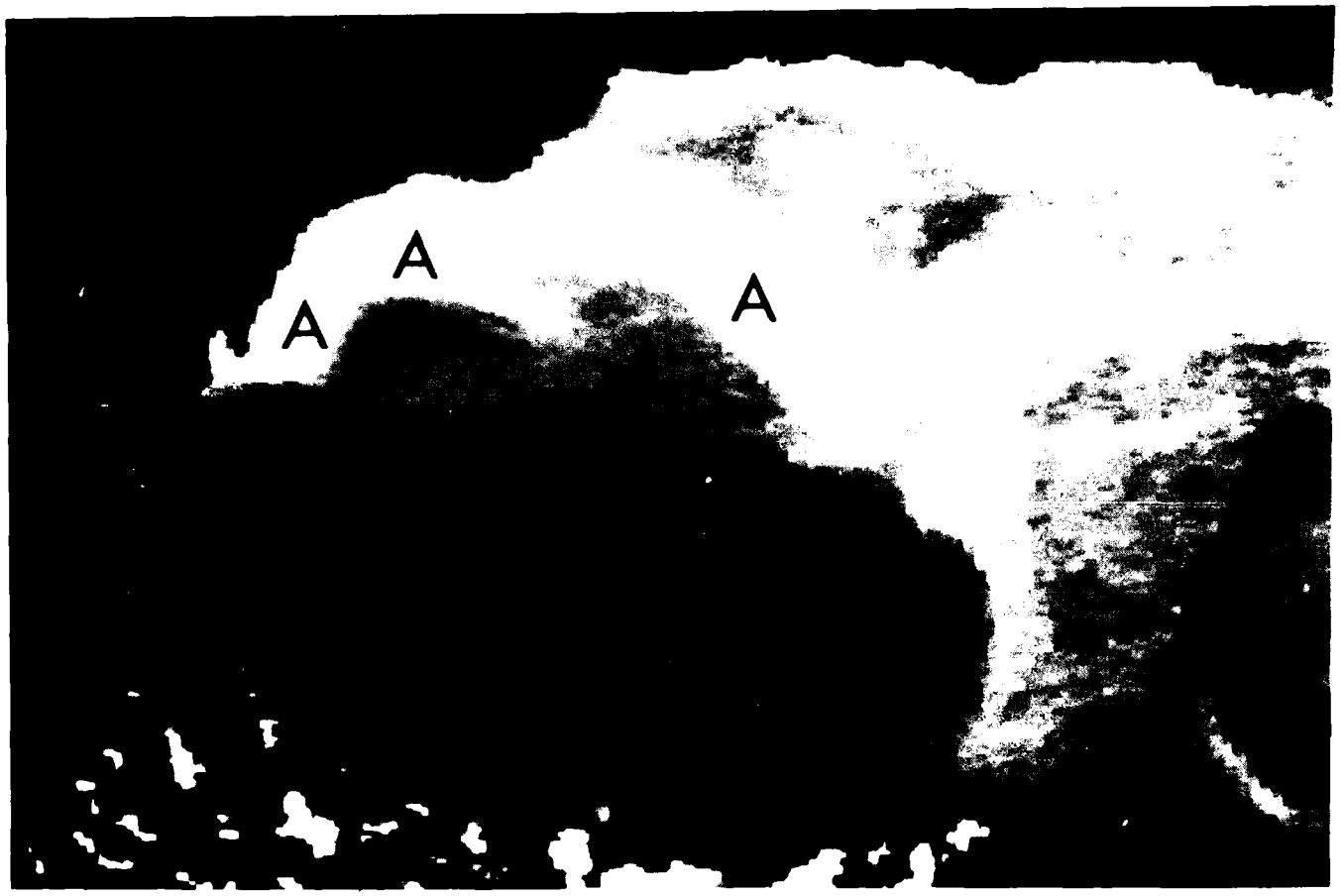
A
A
A

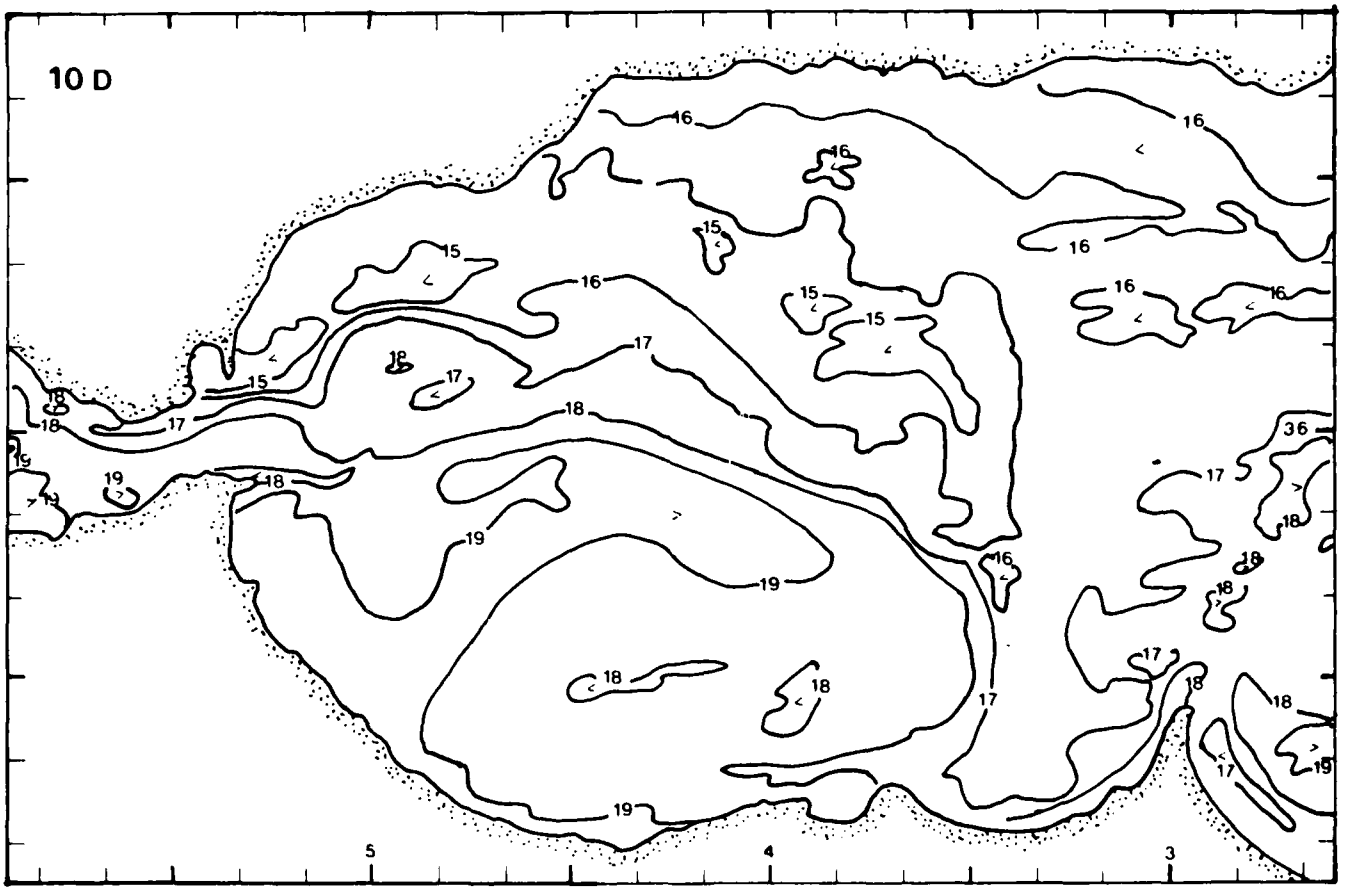
10 D
5
4
3

Figure 30. 11 October 1982, night IR. Apart from the obvious changes observed in the wave-like features associated with the incoming jet, this image is very similar to the previous one. SST are warmer than on 10 October (day). The warmest waters of the "T-like" feature now reach more than 20°C. But the Spanish coastal waters and the coldest waters of the jet remain below 16°C. (Top opposite page.)

Figure 31. SST chart corresponding to the 11 October 1982, night IR image. (Bottom opposite page.)

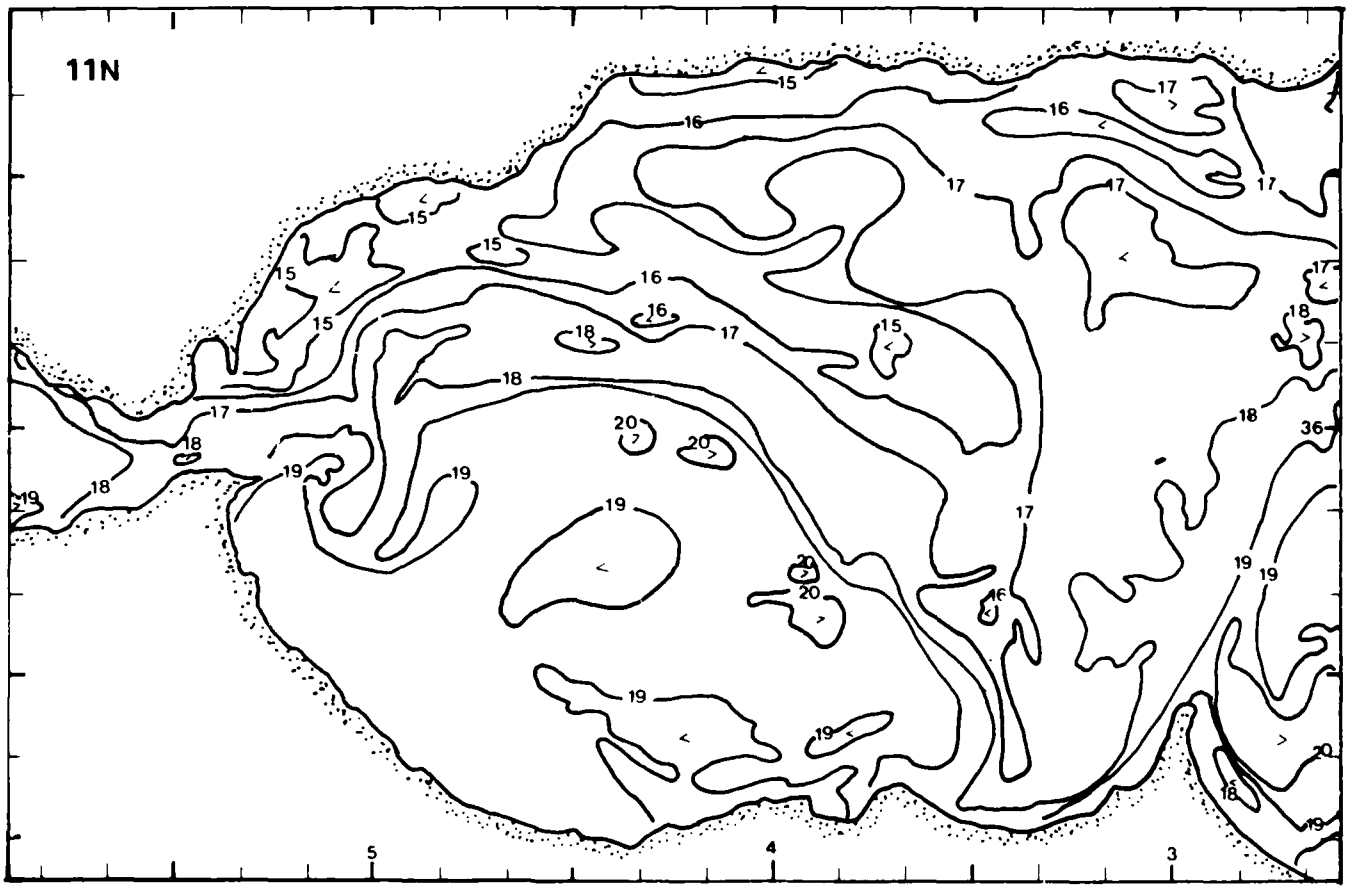
11N
15
16
17
18
19
20
36
5
4
3

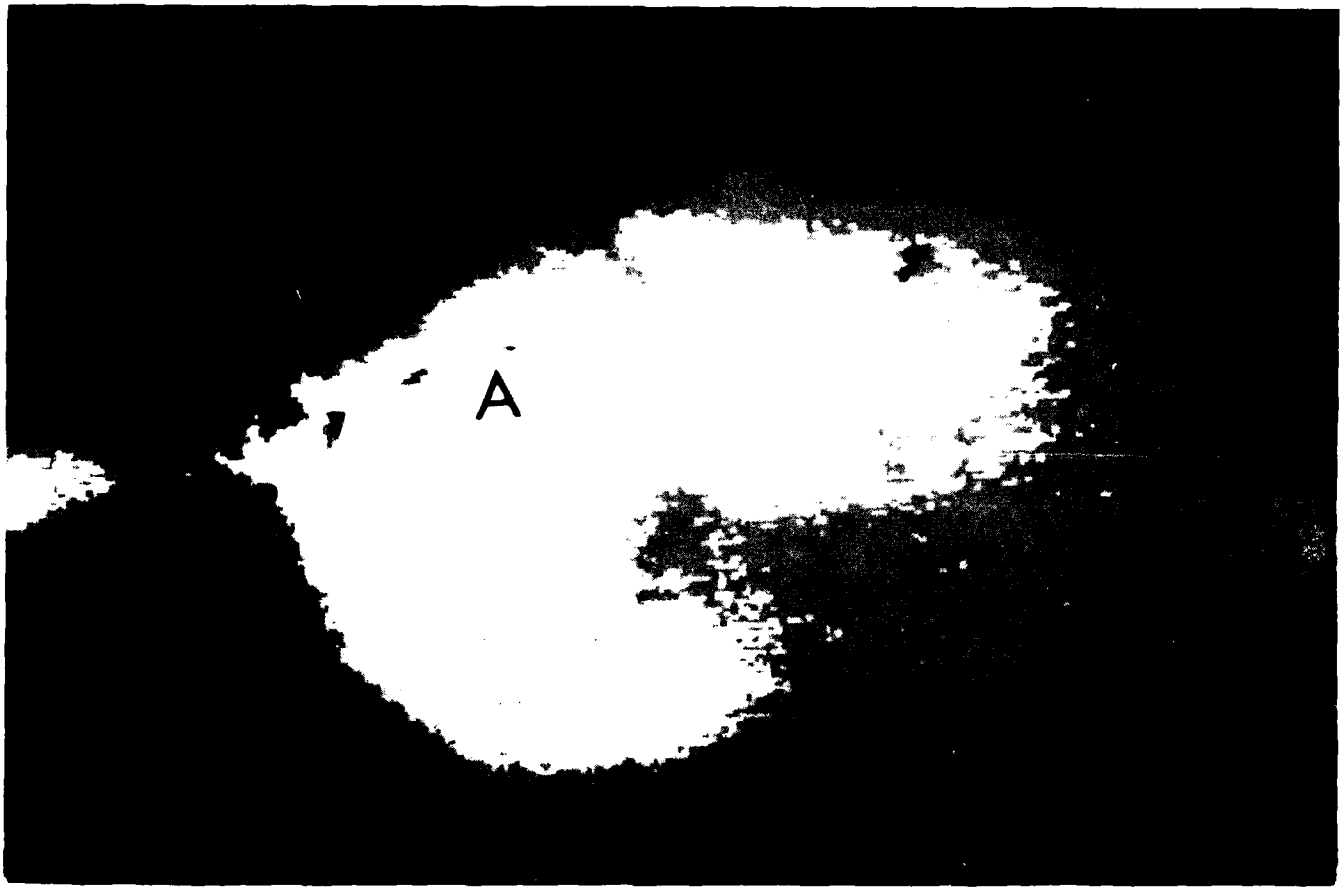

Figure 32. 11 October 1982, day Vis. This visible image is very similar to the 10 October visible image. Notice that the less-reflective area has shifted to the north (A). This may be due to a slight change in wind direction.

Figure 33. 11 October 1982, day IR. SST gradients are weaker than on the previous days, probably due to the continuation of calm wind conditions. The effects of diurnal heating may hide larger subsurface gradients. The front shown at the westernmost A on 10 October (day) has moved eastward to lie immediately to the west of Marbella. (a) SST are increasing to >21°C. The cold temperatures observed in the Marbella area may be due to cloud contamination (see the visible image.). (Top opposite page.)

Figure 34. SST chart corresponding to the 11 October 1982, day IR image. (Bottom opposite page.)

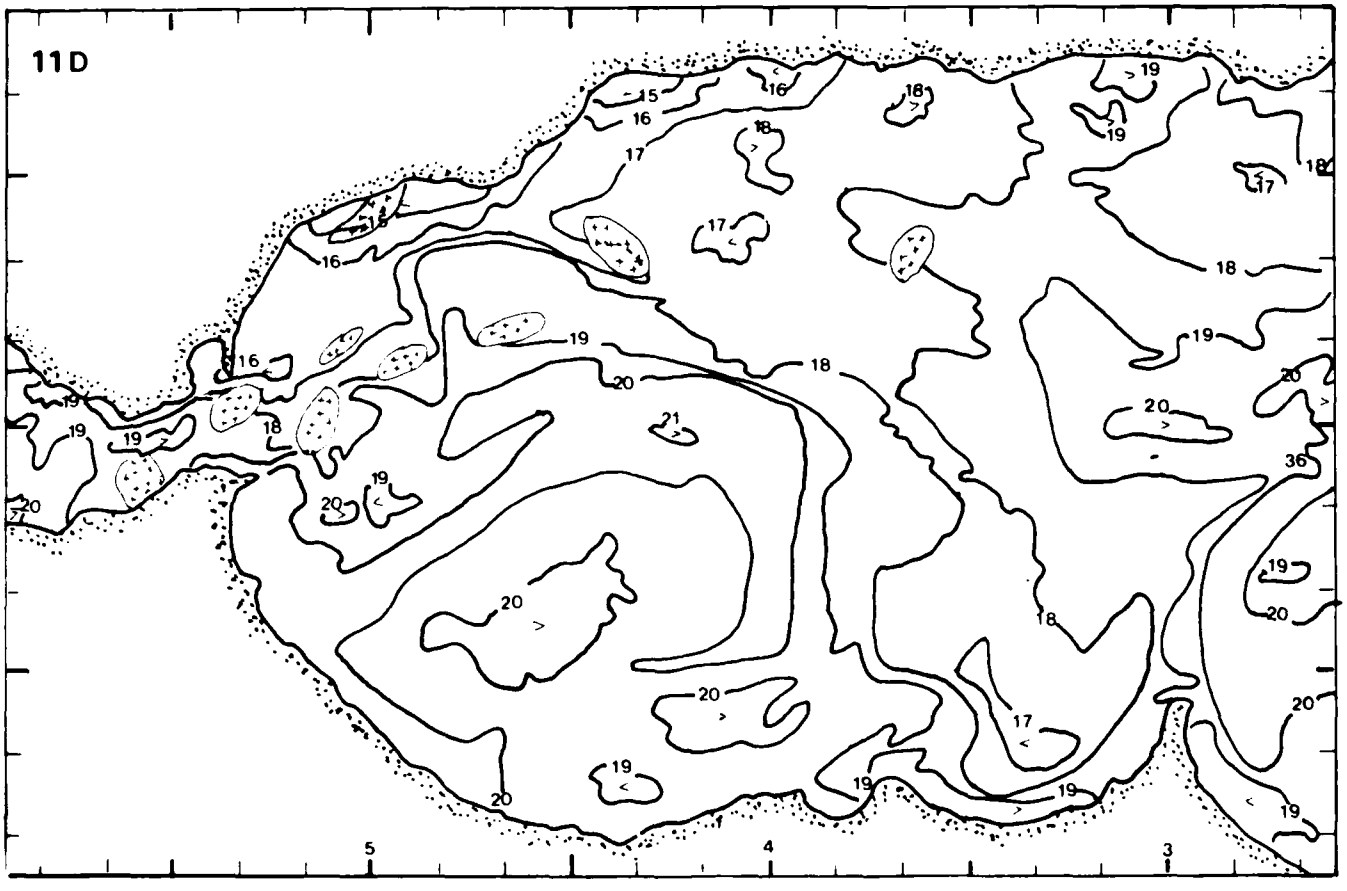
11D
5
4
3

Figure 35. 12 October 1982, night IR. Cloudy. Notice the front at *a* corresponding to the previous image and the extreme northern location of the entire front at *c*.

Figure 36. 12 October 1982, day IR. Cloudy, but an examination of the thermal features shows that there is continuity between the thermal gradients shown in this IR image and the thermal gradients on the previous as well as following IR images. (Top opposite page.)

Figure 37. 12 October 1982, day Vis. (Bottom opposite page.)

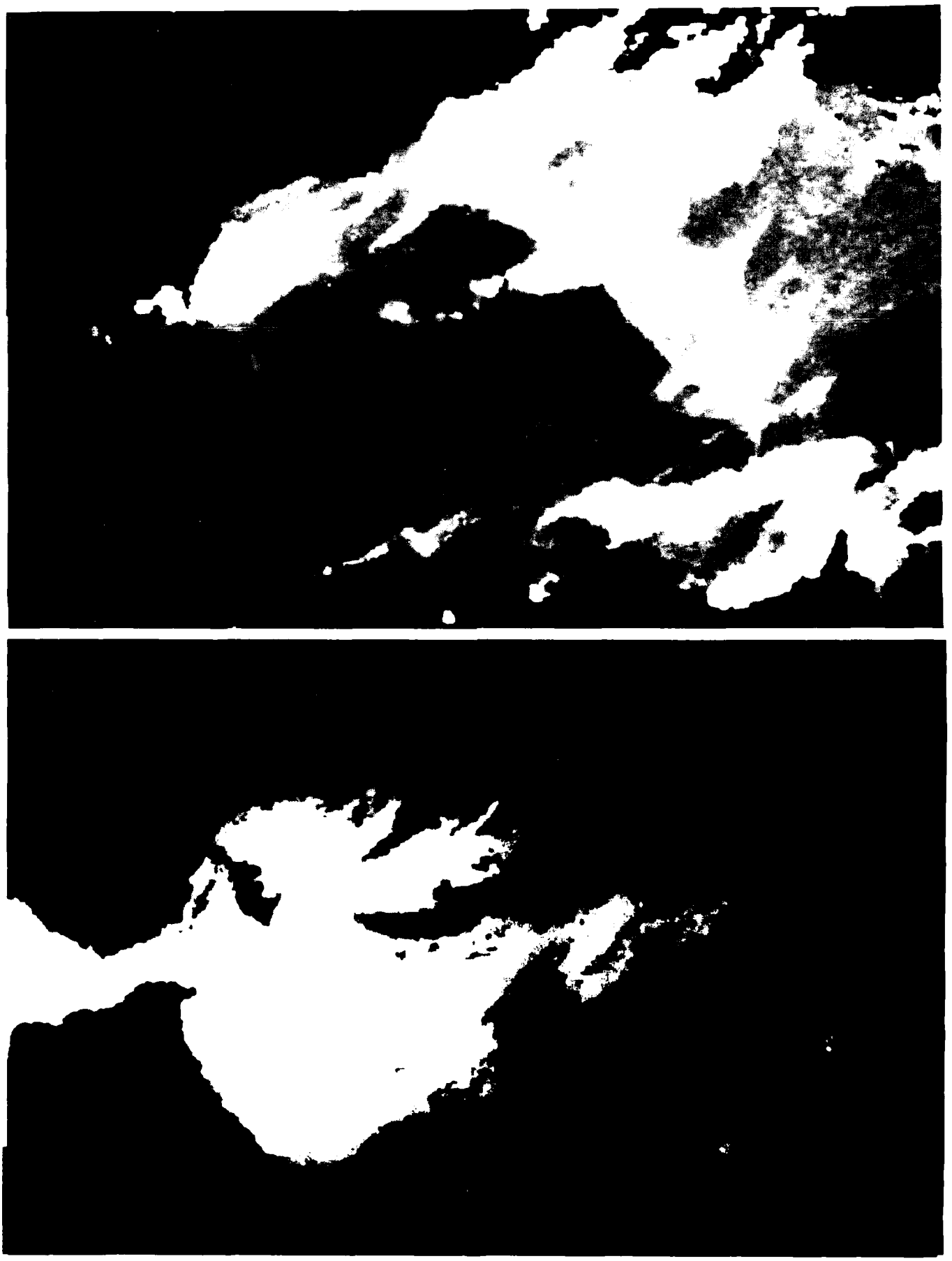

Figure 38. 13 October 1982, night IR. Cloudy. (Top opposite page.)

Figure 39. SST chart corresponding to the 13 October 1982, night IR image. (Bottom opposite page.)

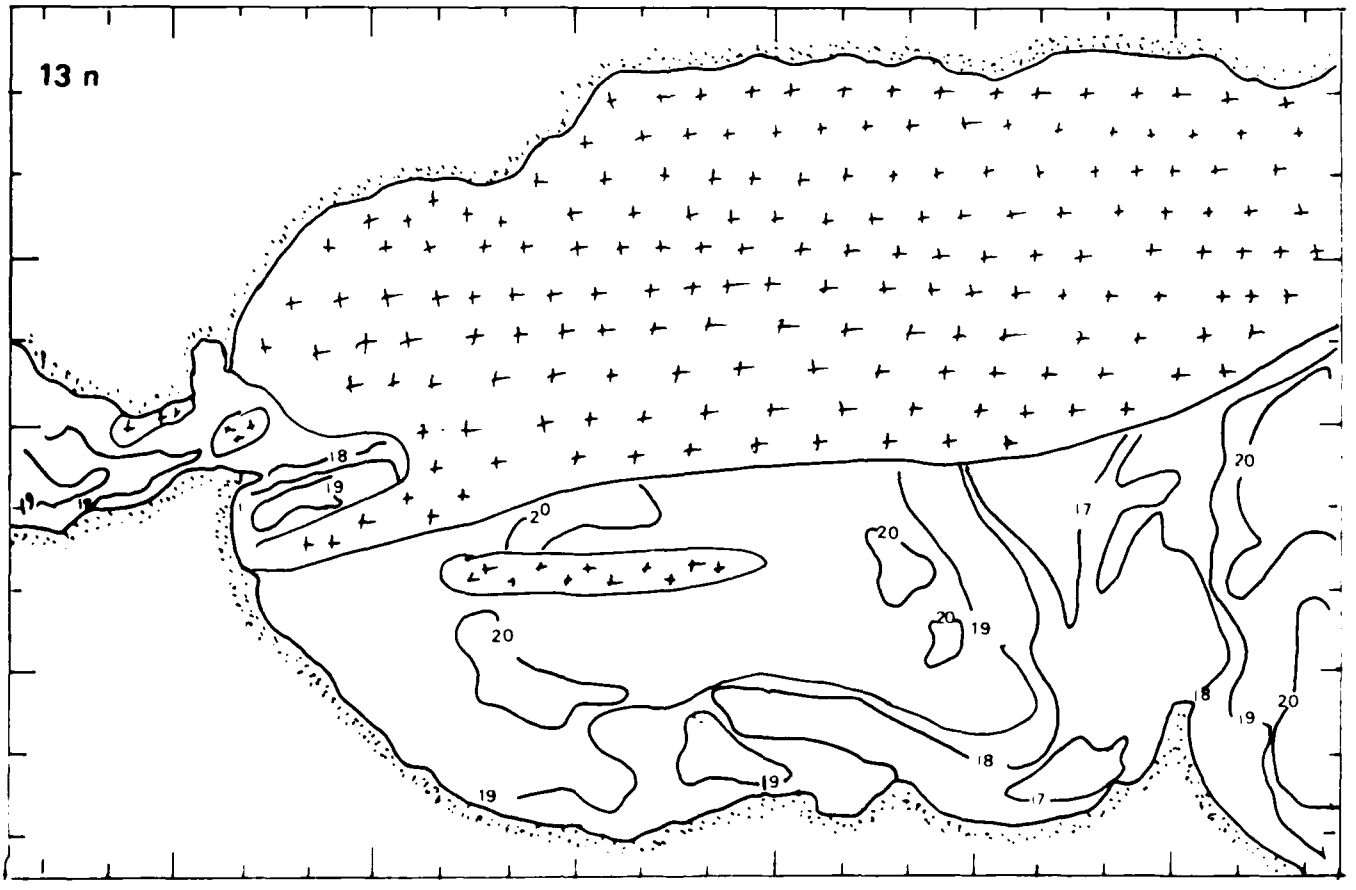
13 n
18
19
19
19
20
20
20
19
20
17
20
19
18
19
19
17
18
19
20

Figure 40. 13 October 1982, day Vis. Apart from the area contaminated by lee-waves, the reflectance picture shows similar patterns to those observed on 10 and 11 October 1982.

Figure 41. 13 October 1982, day IR. In comparing this image to that obtained on 11 October, notice the fronts at *a* and *D*. Temperatures are lower than on 11 October (day) by about 1°C. (Top opposite page.)

Figure 42. SST chart corresponding to the 13 October 1982, day IR image. (Bottom opposite page.)


D.

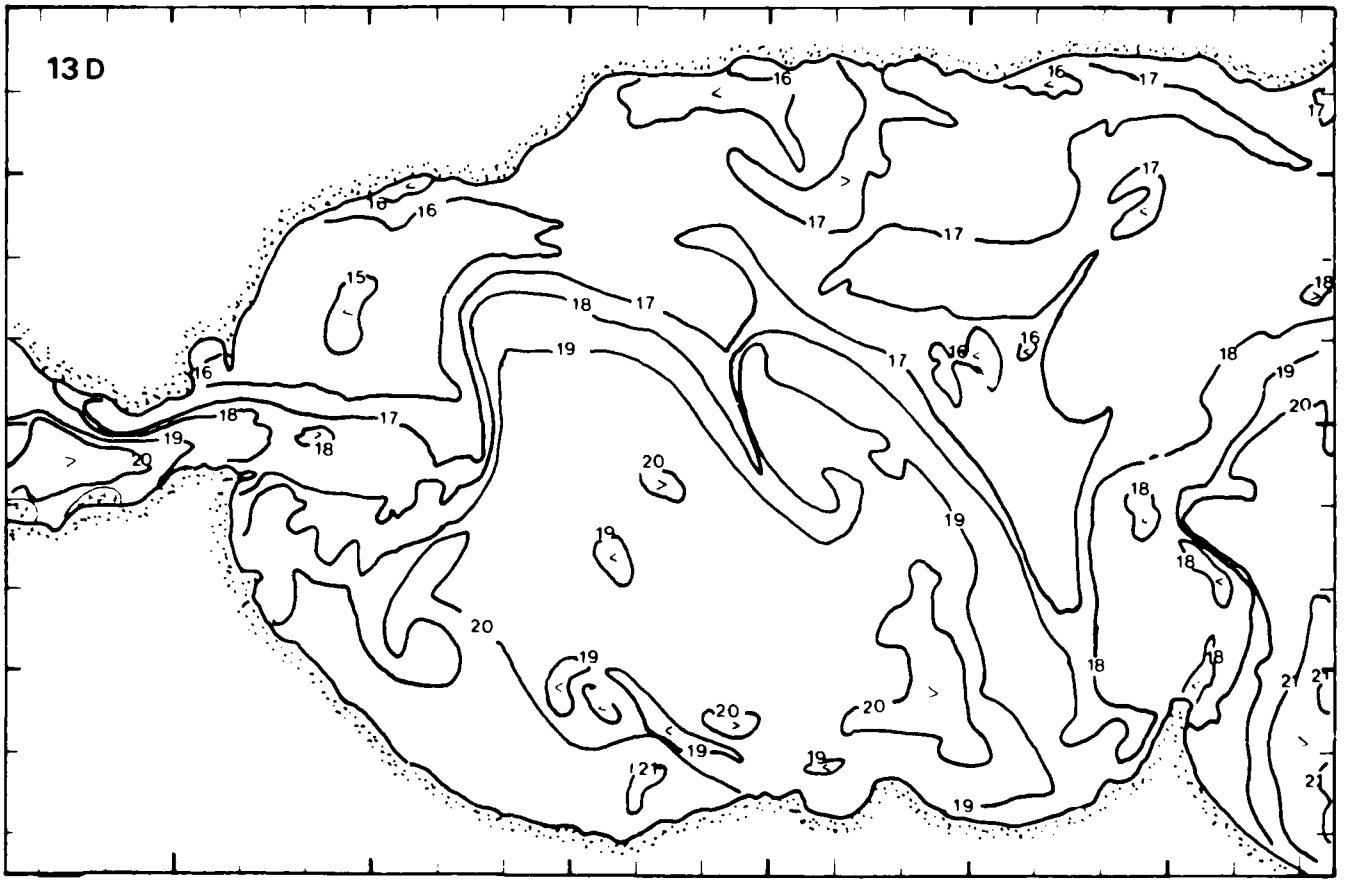
13 D

Figure 43. 14 October 1982, night IR. (Top opposite page.)

Figure 44. 15 October 1982, night IR. Notice the eastward development of the D feature observed on 13 October (day) which has entrapped a warm water tongue between D and E. (Bottom opposite page.)


E
D
E

Figure 45. 16 October 1982, night IR. The temperatures of the Alboran Sea west of the Tres Forcas Cape do not go higher than 19°C. However, temperatures east of the Cape remain high (>20°C). Note that cool temperatures (<15°C) are observed along the Spanish coast. (Top opposite page.)

Figure 46. SST chart correspnding to the 16 October 1982, night IR image. (Bottom opposite page.)


E
D

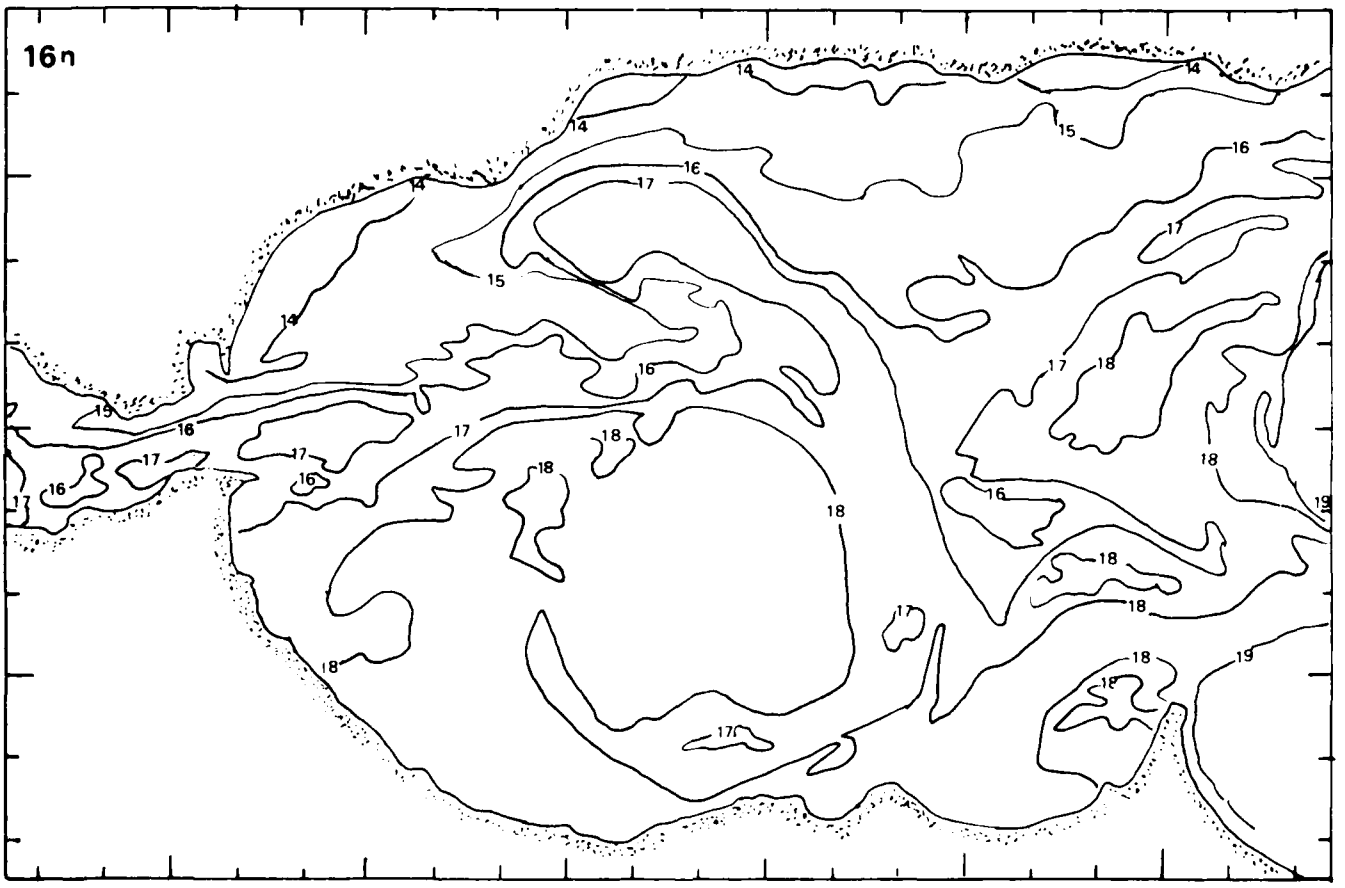
16n
14
15
16
17
18
19

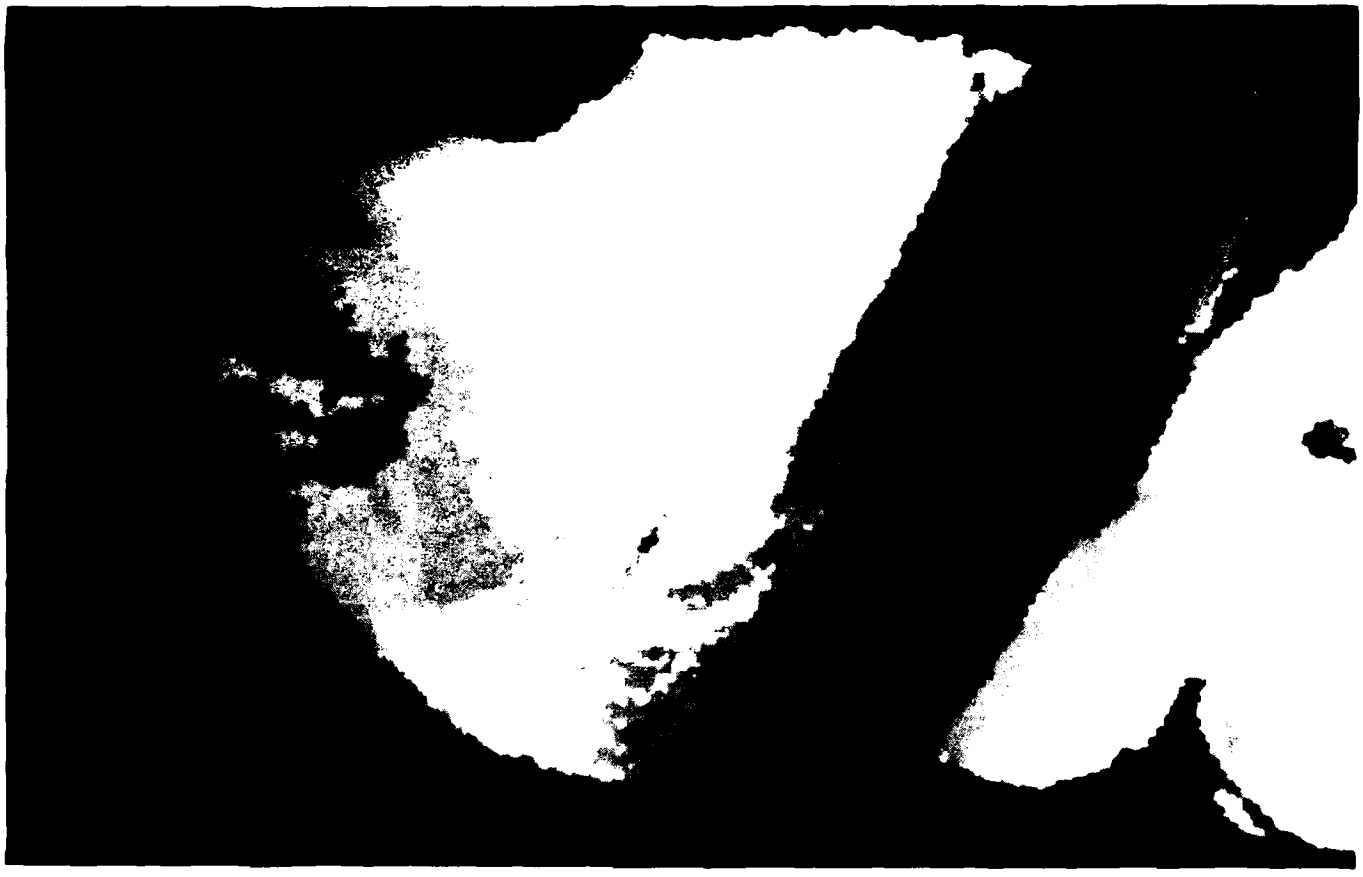

Figure 47. 16 October 1982, day Vis.

Figure 48. 16 October 1982, day IR. SST has risen to 20.5°C in the southwest section of the gyre. Notice the persistence of the warm water that has been almost completely enclosed at *f*. (Top opposite page.)

Figure 49. SST chart corresponding to 16 October 1982 (day) IR image. (Bottom opposite page.)


f

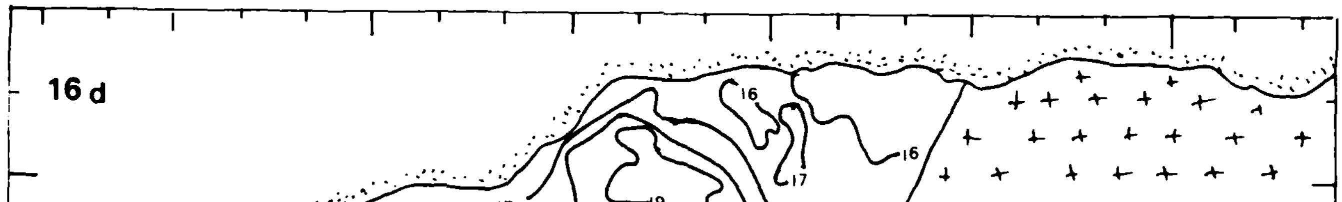
16 d
16
17
18
19
20

Figure 50. 17 October 1982, night IR. (Top opposite page.)

Figure 51. 18 October 1982, night IR. (Bottom opposite page.)

Figure 52. 18 October 1982, day Vis. (Top opposite page.)

Figure 53. 18 October 1982, day IR. (Bottom opposite page.)

Figure 54. 19 October 1982, night IR. Although these last few days present cloudy images, the thermal gradients do show continuity from image to image and close examination can reveal the image to image movement of the gradients. (Top opposite page.)

Figure 55. SST chart corresponding to the 19 October 1982, night IR image. (Bottom opposite page.)

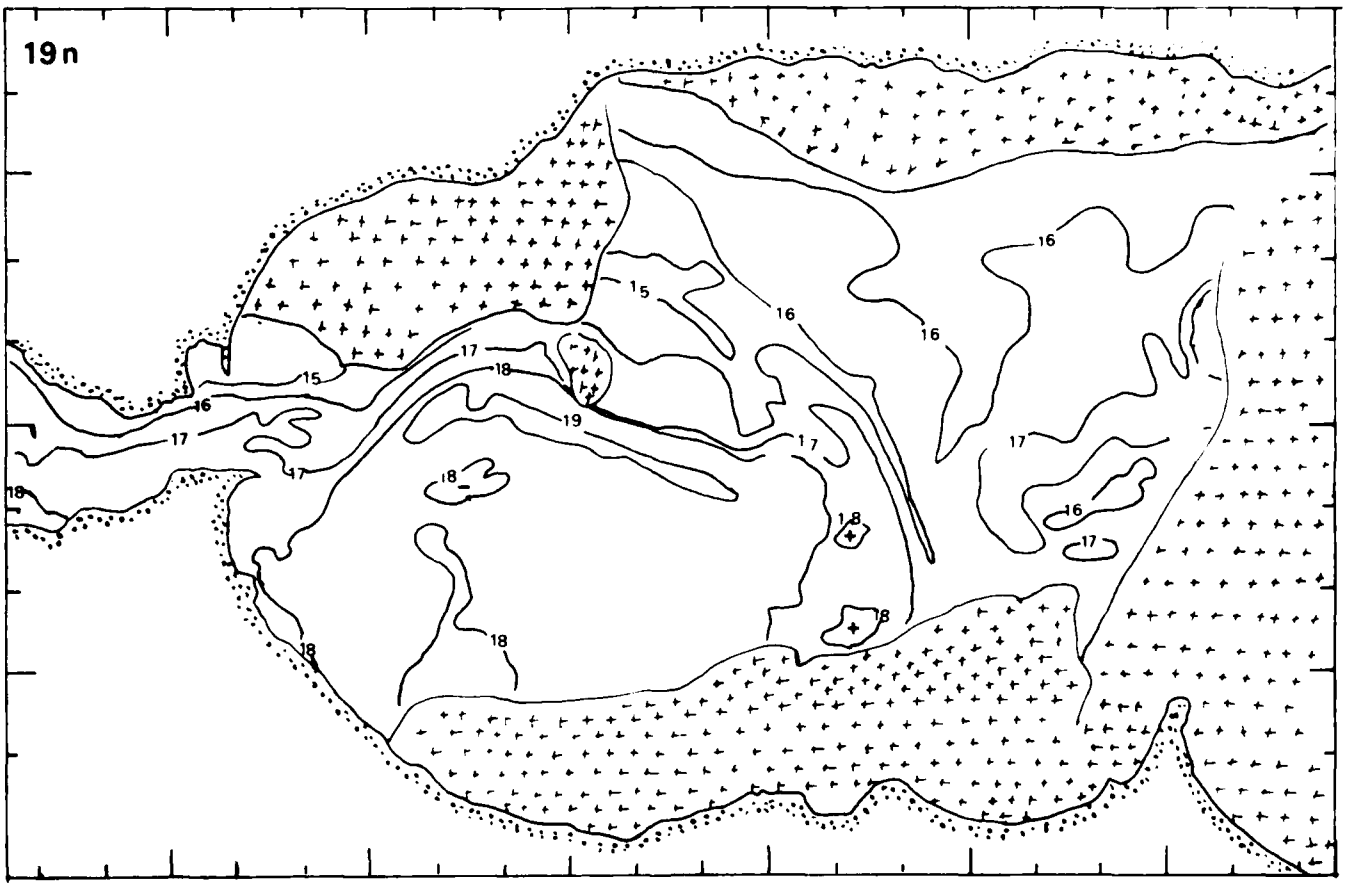
19n
15
16
17
18
19

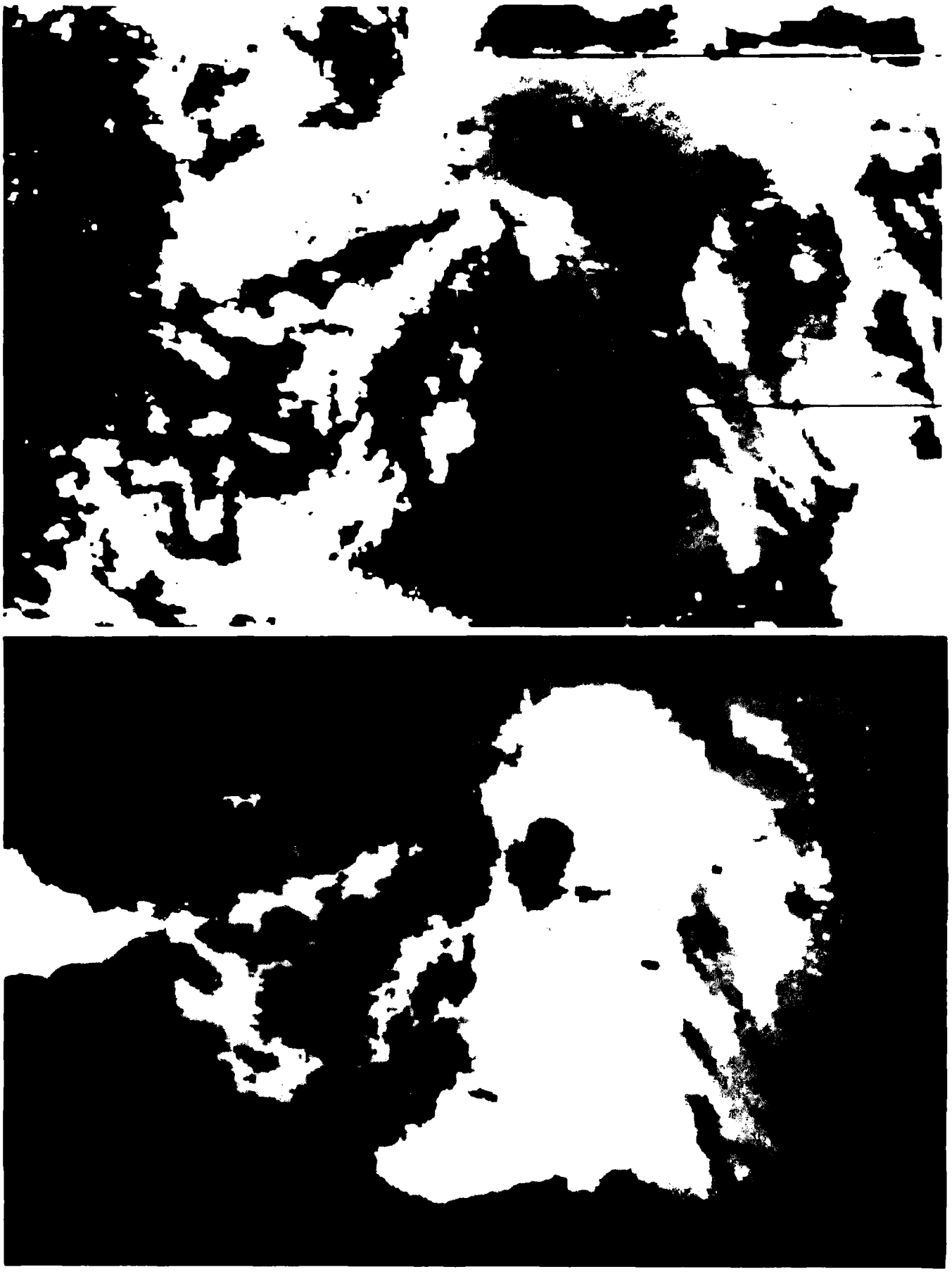

Figure 58. 20 October 1982, night IR.

Figure 56. 19 October 1982, day IR. (Top previous page.)

Figure 57. 19 October 1982, day Vis. (Bottom previous page.)

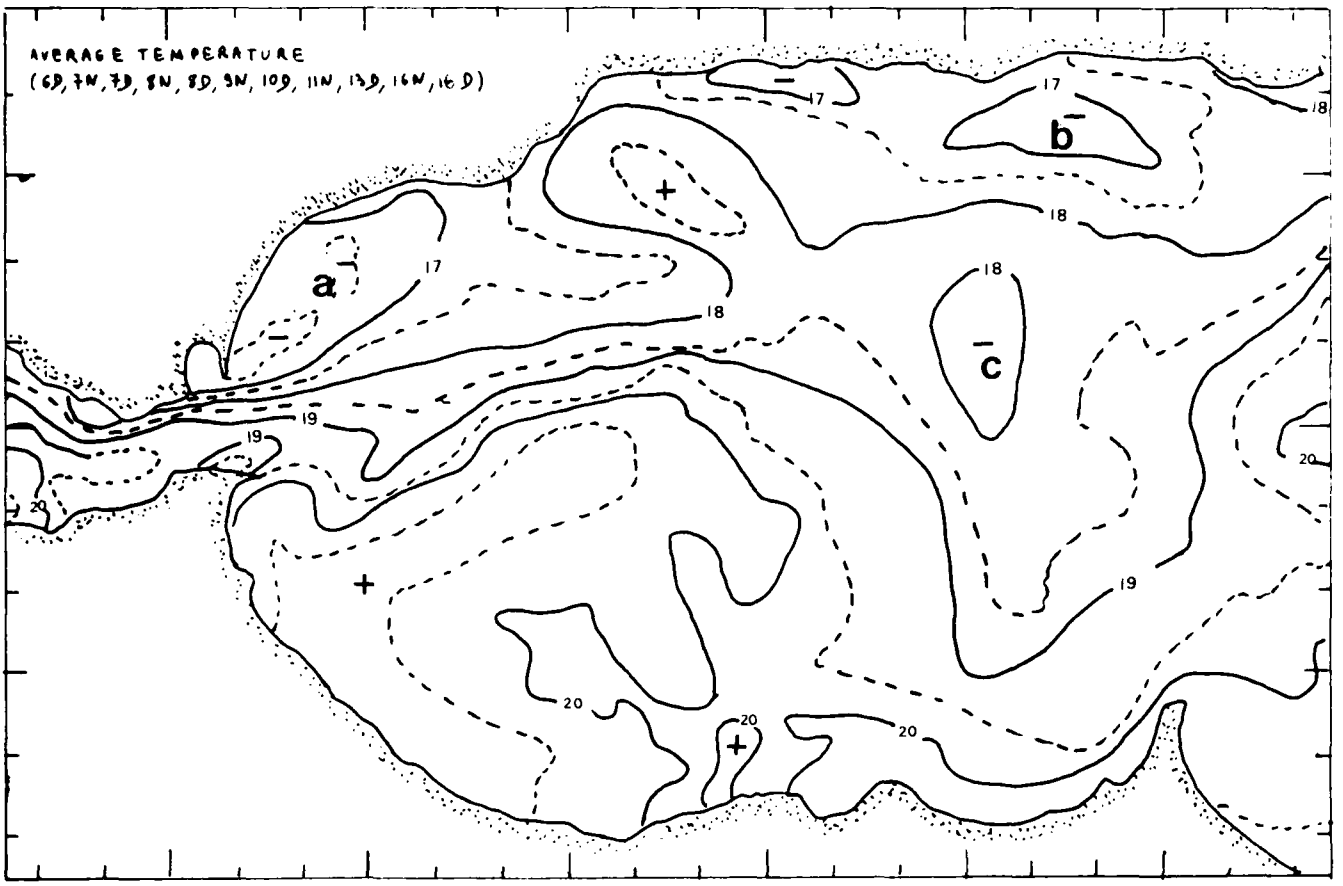

Figure 59. This figure and Figure 60 present examples of the possible computer combinations that may be made with the registered images. This figures gives the average of the SST observed between the 6 October and 16 October, 1982. It shows that two major cold wells persist at (a) and (b) and a secondary cold area at (c). Although, (b) may be due to offshore winds, (a) is probably caused by the strong flow of Atlantic water moving into the Alboran Sea just to the south. This rapid movement may induce upwelling or divergence along the northern edge of the inflowing water and thus causing the cold water found at (a). On the other hand, (c) appears to have a different cause (perhaps bottom topography?). Note that the warmest waters are found in the central and in the southern part of the Alboran anticyclonic eddy.

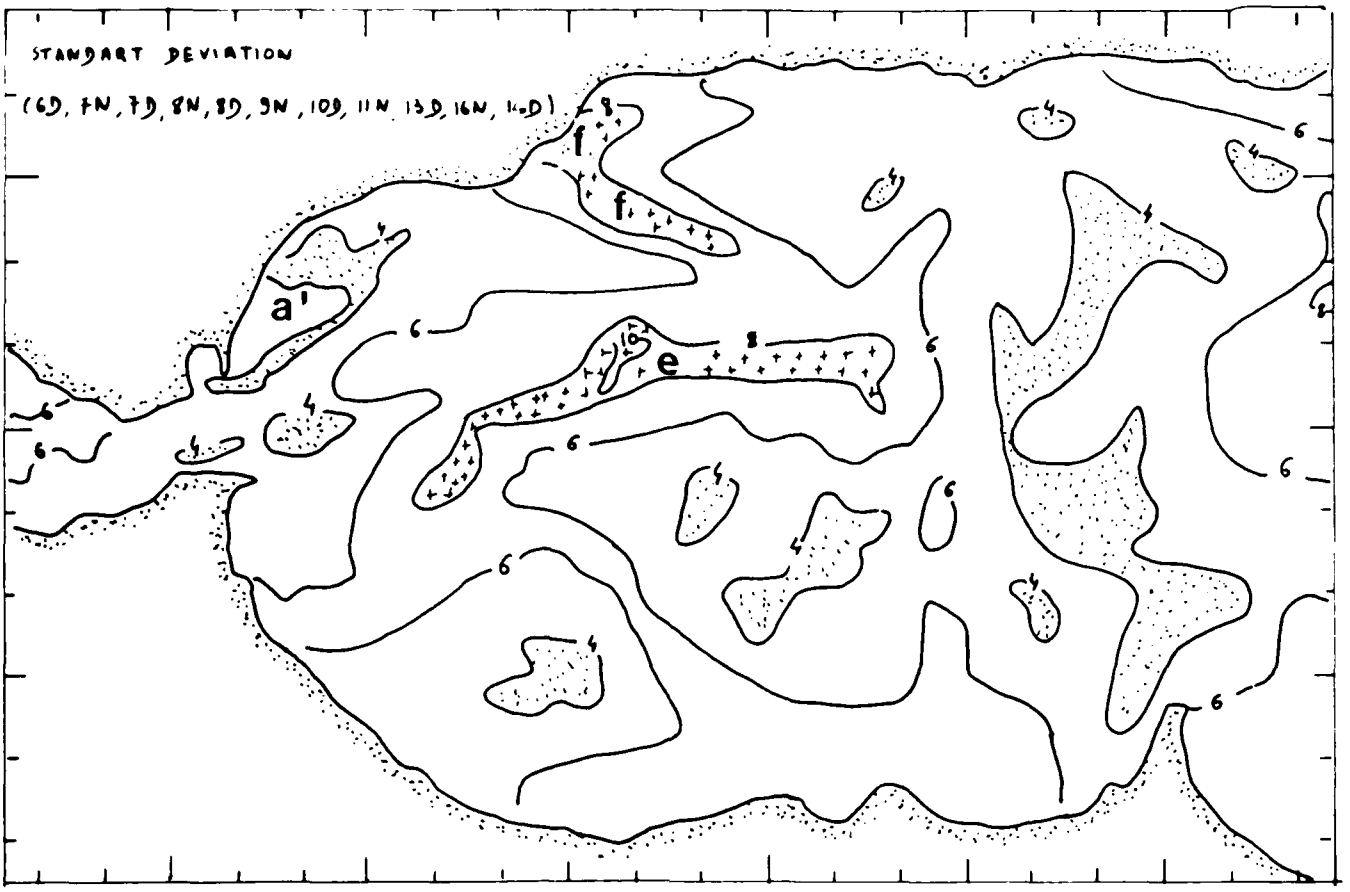

Figure 60. This figure shows that the areas where the temperatures changed the least during the period 6 October through 16 October 1982. (a) here corresponds to the persistent cold water area (a) in Figure 59 and the North-South zone situated at the longitude of the Tres Forcas Cape. Other SST steady areas are found in the Strait of Gibraltar and in some places of the warm core of the Alboran Gyre. Areas where large SST changes occurred are located at (e) (due to the highly variable position of the inflowing Atlantic water) and at (f) (mainly due to the warm feature observed here on 15 and 16 October).

References

Deschamps P. Y. and Phulpin T., 1980: Atmospheric correction of infrared measurements of sea surface temperature using channels at 3.7, 11 and 12 m. Boundary Layer Meteorology, Vol. 18, pp. 131-143.

Hussey, W. J., 1979: *The TIROS-N/NOAA Operational Satellite System*, National Environmental Satellite Service/NOAA, Washington, DC, May, NOAA Tech. Memo. 95, NESS, 35 pp.

La Violette, P. E., 1983: The advection of cyclic submesoscale thermal features in the Alboran Gyre. IUGG Hamberg.

Schwalb, A., 1978: *The TIROS N/NOAA A-G Satellite Series*, National Environmental Satellite Service, NOAA, Washington, DC, March, NOAA Tech. Memo. 95, NESS, 75 pp.

APPENDIX I: Geographic Registration (from R. Holyer)

Geographic registration of AVHRR images consisted of four major steps:

Step 1. Image Navigation

Positioning of the satellite in space is based on ephemeris data obtained from the Naval Space Surveillance Center in Dahlgren, Virginia. Orbital calculations and computer modelling of the AVHRR sensor are combined to derive approximately 250 points within the geographical area of interest where the latitude and longitude of the selected pixels are calculated. These latitude-longitude/sample-line pairs are used as "control points" to define a set of polynomials that transform image coordinates (samples and lines) into geographic coordinates (latitude and longitude).

Step 2. Image Linearization

The pixels in AVHRR images are spaced in the cross-track direction at equal increments of scan angle. Thus, each pixel in a scan line does not represent an equal increment of ground distance due to the varying viewing slant path and earth curvature across the scan line. This equiangular sampling leads to spatial distortion in the images, especially near either end of the scan line. It has been found that the actual "warping" of the image to the desired map projection in Step 3 can be done more precisely if the image is resampled so that each pixel represents a constant increment of ground distance rather than a constant increment of scan angle. This resampling process is called image linearization.

Step 3. Image Warping

In warping the image the polynomials calculated from the control points in Step 1 are applied to the linearized image to generate a warped image that contains the satellite data in a mercator projection. The transformation from satellite image coordinates to mercator geographical coordinates is initially defined in terms of third-order, two-dimensional polynomials. However, to save computational time when actually warping the images, the full polynomial equation is not used. Rather the polynomial is approximated by a piecewise linear equation. This approximation does not introduce any significant error when the image has been linearized first in Step 2.

Step 4. Image Final Shifting

The warped image output from Step 3 typically has positional accuracy of 4-5 km. This accuracy can be improved by finding landmarks of known geographical location and evaluating their position within the warped image. If the fit is not perfect, the warped image can be shifted vertically or horizontally to move the landmarks to their correct positions. If landmarks are available in the image so that this last fine tuning step can be performed, the accuracy of the resulting geographically registered image is generally within 1 km.

APPENDIX II: Split Window Atmospheric Corrections (from T. Phulpin)

1-Summary of Atmospheric Effects:

An approximate equation of the radiative transfer between the sea surface and the satellite is:

$T\lambda = Ts - (1-t)x(Ts-Ta)$ (1)

$T\lambda$:brightness temperature measured by the AVHRR radiometer.
Ts :sea surface temperature.
Ta :equivalent radiative temperature of the atmosphere.
t :total transmittivity of the atmosphere at λ.

The effects of the atmospheric absorption on SST gradients are described, in a first approximation, by:

$T\lambda(A) - T\lambda(B) = (Ts(A) - Ts(B))xt$ (2)

A and B: sea surface points located in an area where the above atmosphere is homogeneous = $Ta(A) = Ta(B)$, $t(A) = t(B) = t$, $Ts(A) \neq Ts(B)$.

Equation 2 shows that the atmosphere attenuates the SST gradients.

Assuming, now, that points A and B are located in an area where the SST is homogeneous $(Ts(A) = Ts(B))$, but where the equivalent temperature of the atmosphere changes $(Ta(A) \neq Ta(B))$, then, an anomalous gradients appears on the satellite SST measurements even in the absence of clouds:

$T\lambda(A) - T\lambda(B) = (1-t)x\Delta Ta$ (3)

with $\Delta Ta = Ta(A) - Ta(B)$.

An anomalous SST gradient also appears if differences exist in the water vapor content between A and B inducing a change in t between these two points $(Ts(A) = Ts(B), Ta(A) = Ta(B), t(A) \neq t(B))$.

$T\lambda(A) - T\lambda(B) = (Ts - Ta)x\Delta t$ (4)

with $\Delta t = t(A) - t(B)$

Equations 3 and 4 show that changes in the composition of a cloud-free atmosphere may induce anomalous gradients on SST images.

2-Split Window Atmospheric Corrections:

Removing effects of atmospheric absorption from IR measurements is possible using combinations of two (3.7-11 μm, 3.7-12 μm, 11-12 μm) or three (3.7-11-12 μm) AVHRR channels.

Because the 3.7 μm channel of the NOAA-7 AVHRR is noisy and because its daylight measurements are contaminated by solar radiations, we have chosen to correct the ¿Donde Va? data using the split-window combination (11-12 μm).

According to the theoretical studies achieved by Deschamps and Phulpin in France and by other scientists in the United States (see MacClain papers) the equation of correction is:

$Ts = a + bxT11 + cxT12$

with Ts = sea surface temperature
a = constant taking into account all the effects neglected in the linear regression: solar reflection, absorption by minor atmospheric components, radiometer bias.

It is assumed that the absorption is mainly due to the water vapor content of the atmosphere.

The constants b and c are related by:

$$b = \frac{1+t12}{t11-12} \qquad c = \frac{1+t11}{t11-t12} \qquad and\ b + c = 1$$

$b / c = \alpha 11 / \alpha 12$ *assuming* $t\lambda = 1 - \alpha\lambda xw$,
w = water vapor content of the atmosphere.
λ = wavelength of the measurement.

First, b and c were computed using simulations of the atmospheric transmittance through various climatological conditions (MacClain, Phulpin). Results from such theoretical computations are very similar. For example MacClain gives the following result:

$Ts = -76 + 3.93xT11 - 2.93xT12$ *(in °C)*

Another method has been used by T. Phulpin at CMS. He has experimentally chosen the values of *b* and *c* that remove from fine resolution enhanced images the atmospheric effects obviously due to an increase of the water vapor content of the atmosphere without cloud formation. Images showing atmospheric lee-waves were used to this purpose.

The following figures give an idea of the method used:

The best value of *b/c* to remove absorption effects was found to be 0.66. Consequently taking into account the relationship $b + c = 1$, *b* was chosen to equal 3 and *c* to equal -2. Applied to a CMS file of NOAA-7 validation data (BERTHE2 about 70 points located in the NE Atlantic and in the Mediterranean) this algorithm with a value for *a* of 0.5° C (qualitatively determined using a few points of comparison in the Atlantic) gives a bias of 0.11° C (which have to be added to the *a* constant) and a standard deviation of 0.40° C.

This algorithm has been applied to the ?Donde Va? data to obtain the images and charts presented in this report. Notice that the calibration of IR data was made at NORDA using a method slightly different from the one used at CMS (for instance to calibrate the BERTHE2 data). NORDA used the plank's function applied to the central wavelength adjusted for each IR channel at the temperature of 300° K. Taking into account that this central wavelength varies with the temperature, we at CMS prefer to use a calibration table for converting radiances into temperatures. A table is computed for each IR channel using the transfer function of each channel window. This difference in calibration methods may induce a slight bias in the ?Donde Va? corrected data because the algorithm used was adjusted to data calibrated at CMS.

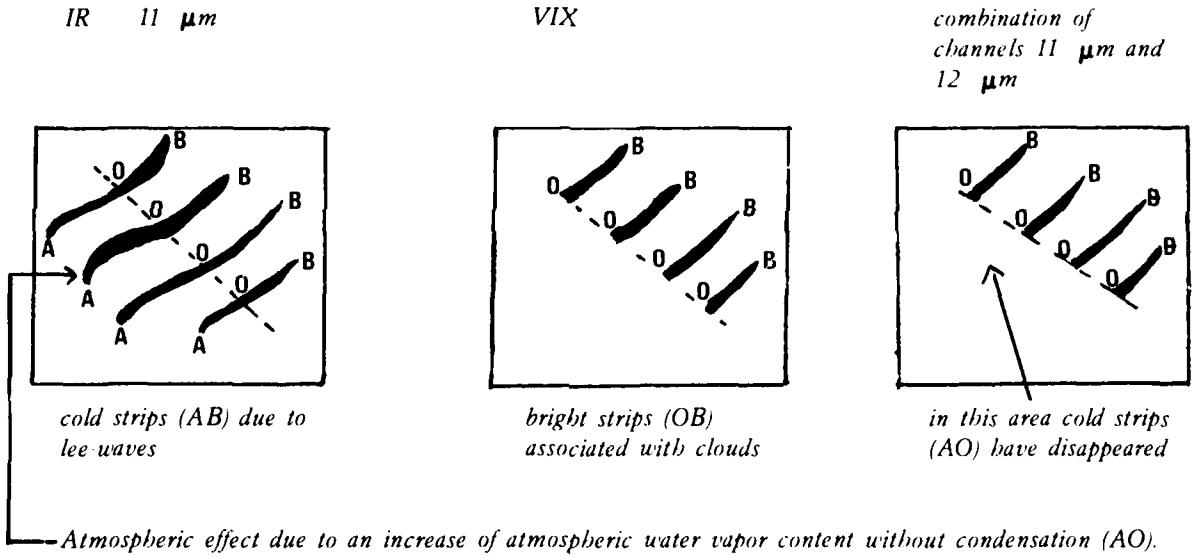

Distribution List

Department of the Navy
Asst Deputy Chief of Navy Materials
for Laboratory Management
Rm 1062 Crystal Plaza Bldg 5
Washington DC 20360

Department of the Navy
Asst Secretary of the Navy
(Research Engineering & System)
Washington DC 20350

Project Manager
ASW Systems Project (PM-4)
Department of the Navy
Washington DC 20360

Department of the Navy
Chief of Naval Material
Washington DC 20360

Department of the Navy
Chief of Naval Operations
ATTN: OP 951
Washington DC 20350

Department of the Navy
Chief of Naval Operations
ATTN: OP 952
Washington DC 20350

Department of the Navy
Chief of Naval Operations
ATTN: OP 987
Washington DC 20350

Director
Chief of Naval Research
ONR Code 420
Ocean Science & Technology Det
NSTL, MS 39529

Director
Defense Technical Info Cen
Cameron Station
Alexandria VA 22314

Commander
DW Taylor Naval Ship R&D Cen
Bethesda MD 20084

Commanding Officer
Fleet Numerical Ocean Cen
Monterey CA 93940

Director
Korean Ocean R&D Inst
ATTN: K. S. Song, Librarian
P. O. Box 17 Yang Jae
Seoul South Korea

Commander
Naval Air Development Center
Warminster PA 18974

Commander
Naval Air Systems Command
Headquarters
Washington DC 20361

Commanding Officer
Naval Coastal Systems Center
Panama City FL 32407

Commander
Naval Electronic Sys Com
Headquarters
Washington DC 20360

Commanding Officer
Naval Environmental Prediction
Research Facility
Monterey CA 93940

Commander
Naval Facilities Eng Command
Headquarters
200 Stovall St.
Alexandria VA 22332

Commanding Officer
Naval Ocean R & D Activity
ATTN: Code 110
Code 125
Code 200
Code 300
Code 115
NSTL MS 39529

Director
Liaison Office
Naval Ocean R & D Activity
800 N. Quincy Street
502 Ballston Tower #1
Arlington VA 22217

Commander
Naval Ocean Systems Center
San Diego CA 92152

Commanding Officer
Naval Oceanographic Office
NSTL MS 39522

Commander
Naval Oceanography Command
NSTL MS 39522

Superintendent
Naval Postgraduate School
Monterey CA 93940

Commanding Officer
Naval Research Laboratory
Washington DC 20375

Commander
Naval Sea System Command
Headquarters
Washington DC 20362

Commander
Naval Surface Weapons Center
Dahlgren VA 22448

Commanding Officer
Naval Underwater Systems Center
ATTN: New London Lab
Newport RI 02840

Director
New Zealand Oceano Inst
ATTN: Library
P. O. Box 12-346
WELLINGTON N., NEW ZEALAND

Director
Office of Naval Research
Ocean Science & Technology Div
NSTL MS 39529

Department of the Navy
Office of Naval Research
ATTN: Code 102
800 N. Quincy St.
Arlington VA 22217

Commanding Officer
ONR Branch Office
536 S Clark Street
Chicago IL 60605

Commanding Officer
ONR Branch Office LONDON
Box 39
FPO New York 09510

Commanding Officer
ONR Western Regional Ofs
1030 E. Green Street
Pasadena CA 91106

President
Texas A&M
ATTN: Dept of Ocean Working Collection
College Station TX 77843

Director
University of California
Scripps Institute of Oceanography
P. O. Box 6049
San Diego Ca 92106

Director
Woods Hole Oceanographic Inst
Woods Hole MA 02543

UNCLASSIFIED

SECURITY CLASSIFICATION OF THIS PAGE *(When Data Entered)*

REPORT DOCUMENTATION PAGE		READ INSTRUCTIONS BEFORE COMPLETING FORM
1. REPORT NUMBER NORDA Report 65	2. GOVT ACCESSION NO. AD-A163407	3. RECIPIENT'S CATALOG NUMBER
4. TITLE *(and Subtitle)* NOAA-7 AVHRR IMAGES OBTAINED DURING THE DONDE VA? EXPERIMENT IN THE ALBORAN SEA, 1 THROUGH 20 OCTOBER 1982		5. TYPE OF REPORT & PERIOD COVERED Final 6. PERFORMING ORG. REPORT NUMBER
7. AUTHOR(s) Michele Champagne-Philippe Paul E. La Violette		8. CONTRACT OR GRANT NUMBER(s)
9. PERFORMING ORGANIZATION NAME AND ADDRESS Naval Ocean Research and Development Activity Ocean Science Directorate NSTL, Mississippi 39529		10. PROGRAM ELEMENT, PROJECT, TASK AREA & WORK UNIT NUMBERS
11. CONTROLLING OFFICE NAME AND ADDRESS Same		12. REPORT DATE February 1984 13. NUMBER OF PAGES 56
14. MONITORING AGENCY NAME & ADDRESS *(if different from Controlling Office)*		15. SECURITY CLASS. *(of this report)* UNCLASSIFIED 15a. DECLASSIFICATION/DOWNGRADING SCHEDULE

16. DISTRIBUTION STATEMENT *(of this Report)*

Approved for Public Release
Distribution Unlimited

17. DISTRIBUTION STATEMENT *(of the abstract entered in Block 20, if different from Report)*

18. SUPPLEMENTARY NOTES

19. KEY WORDS *(Continue on reverse side if necessary and identify by block number)*

Alboran Sea NOAA-7
Synoptic Thermal Coverage
Advanced Very High Resolution Radiometer (AVHRR)

20. ABSTRACT *(Continue on reverse side if necessary and identify by block number)*

During the period 1 through 20 October 1982, NOAA-7 satellite data were received and archived at Centre de Meteorologie Spatiale (CMS), Lannion, France. These data were collected as part of the multi-platform international experiment called Donde Va?. The scientific purpose of the satellite data collection was to provide synoptic thermal coverage of the Alboran Sea particularly in the region of the incoming Atlantic water near the Strait of Gibraltar. This report presents comparatively cloud-free images for use as an aide in the analysis of Donde Va? multi-platform data collected by other members of the Donde Va? investigative

DD FORM 1 JAN 73 1473 EDITION OF 1 NOV 65 IS OBSOLETE
S N 0102-LF-014-6601

UNCLASSIFIED
SECURITY CLASSIFICATION OF THIS PAGE *(When Data Entered)*

team. All of the images presented are registered to a mercator projection. In addition, the infrared images have been atmospherically corrected to minimize the effects of atmospheric moisture. The visible images have been enhanced to show sea surface roughness and turbidity changes.